To the Graduate Council:

I am submitting herewith a thesis written by Joseph A. M. Boulet entitled "Coupled Structural Response to a Three Component Seismic Disturbance." I recommend that it be accepted in partial fulfillment of the requirements for the degree of Master of Science, with a major in Engineering Science.

Thomas G. Carley

Thomas G. Carley, Major Professor

We have read this thesis
and recommend its acceptance:

William J. Snyder

Bruce R Ewey

Accepted for the Council:

Dillon A. Smith

Vice Chancellor
Graduate Studies and Research

COUPLED STRUCTURAL RESPONSE TO A THREE COMPONENT SEISMIC DISTURBANCE

A Thesis

Presented for the

Master of Science

Degree

The University of Tennessee, Knoxville

Joseph A. M. Boulet

August 1976

1287925

To Paula

ACKNOWLEDGMENTS

The author is grateful to Dr. T. G. Carley for his invaluable guidance, and to Paula Renfro for her faithful typing of the manuscript.

ABSTRACT

The purpose of this study was to evaluate several response spectrum analysis techniques for approximating maximum structural displacements in response to seismic ground motion having three spatial components.

For a given structural model and seismic input, maximum structural displacements were taken from a time history computed by numerical integration of the equations of motion. These results were used as a standard against which to compare the various response spectrum analysis techniques.

The primary conclusion of this study is that none of the response spectrum analysis methods tested is consistently accurate.

TABLE OF CONTENTS

SECTION		PAGE
I.	INTRODUCTION.	1
II.	FORMULATION OF THE PROBLEM.	2
	Structural Model.	2
	Equations of Undamped Free Vibration-- Lagrange's Equations.	6
	Eigenvalue Problem.	18
	Equations of Undamped Vibration with Ground Motion	19
	Equations of Damped Vibration with Ground Motion	21
	Modal Analysis.	23
III.	SOLUTIONS TO THE PROBLEM.	25
	Time History Analysis	25
	Response Spectrum Analysis.	25
IV.	NUMERICAL DATA AND PROCEDURES	32
	Structural Data	32
	Eigenvalue Problem.	32
	Excitation.	35
	Time History Analysis	35
	Response Spectrum Analysis.	36
V.	RESULTS AND CONCLUSIONS	38
	Eigenvalue Problem.	38
	Response Spectrum Generation.	38
	Comparison of Response Spectrum Methods	50
	Conclusions	56
LIST OF REFERENCES.		58
APPENDIX.		60
VITA.		68

LIST OF TABLES

TABLE		PAGE
1.	Structural Mass Data.	33
2.	Stiffness Data for Elastic Elements	34
3.	Stiffness Data for Base Springs	34
4.	Natural Frequencies and Modal Participation Factors	39
5.	Mode Shapes 1-3	40
6.	Mode Shapes 4-6	41
7.	Mode Shapes 7-9	42
8.	Mode Shapes 10-12	43
9.	Mode Shapes 13-15	44
10.	Mode Shapes 16-18	45
11.	Mode Shapes 19-21	46
12.	Absolute Sum Results.	51
13.	Square Root of Sum of Squares Results	52
14.	Double Sum Results.	53
15.	Closely Spaced Modes Results.	54
16.	Lin's Method Results.	55

LIST OF FIGURES

FIGURE		PAGE
1.	Structural Model.	3
2.	Typical Mass Element.	4
3.	Typical Elastic Element	5
4.	System Coordinates.	7
5.	Mass Matrix	13
6.	Structural Stiffness Matrix	14
7.	Element Stiffness Matrix.	15
8.	Response Spectrum for $\ddot{x}_g$	47
9.	Response Spectrum for $\ddot{y}_g$	48
10.	Response Spectrum for $\ddot{z}_g$	49

I. INTRODUCTION

Dynamic structural analysis generally requires a well-defined structural model and a time history of the excitation for which the structure is to be designed. Given these, the maximum structural response can be found. In the case of seismic analysis, however, the design excitation is usually expressed as a ground motion response spectrum. The only information provided by a response spectrum is the maximum responses of a family of single degree of freedom systems. Therefore, in order to use a response spectrum for analysis of a multiple degree of freedom system, the equations of motion must be put into the form of independent, single degree of freedom equations. Under certain conditions, this can be accomplished through a coordinate transformation--from system coordinates to modal coordinates. Response spectrum analysis then gives the maximum values of the modal coordinates. But no functional relationship exists between the maximum values of the modal coordinates and the maximum values of the system coordinates. Hence, the maximum structural response cannot be computed.

Although response spectrum analysis does not permit the calculation of the maximum system response, it can be used to approximate that response. Many methods for doing this approximation are discussed in the literature.[1,2] The work discussed herein is a comparison and evaluation of several of these methods, as applied to the same structural model with seismic excitation having three spatial components.

II. FORMULATION OF THE PROBLEM

Structural Model

The structural model was developed by Dr. T. G. Carley, Associate Professor of Engineering Science and Mechanics, the University of Tennessee, Knoxville, and represents a linear system. For this study, the model includes five lumped masses (floors) connected by four elastic members arranged as shown in Fig. 1. The base is supported by three translational springs and two horizontal torsional springs. (Rotation about the vertical axis is not considered for the base mass.) A typical mass element is shown in Fig. 2 with the origin of the coordinate system located at the shear center (elastic axis). The shear center is the only point where horizontally applied forces induce no twisting in the structure. In general, the mass center and shear center of a building floor are distinct locations. Hence, inertia forces, which act at the mass center (see Fig. 2), induce twisting in the structure. Through this induced torsion, the lateral (x and y) displacements of the mass elements are coupled.

The elastic elements are prismatic beams, characterized by bending, transverse shear, and torsional stiffnesses. The beams are connected to the mass elements at the latter's shear centers. A typical beam element is shown in Fig. 3.

The inertia forces generated by the independent rocking (rotation about horizontal axes) of the upper four mass elements are considered insignificant relative to the other forces in the system. Therefore, only 21 degrees of freedom are of interest, as indicated by the

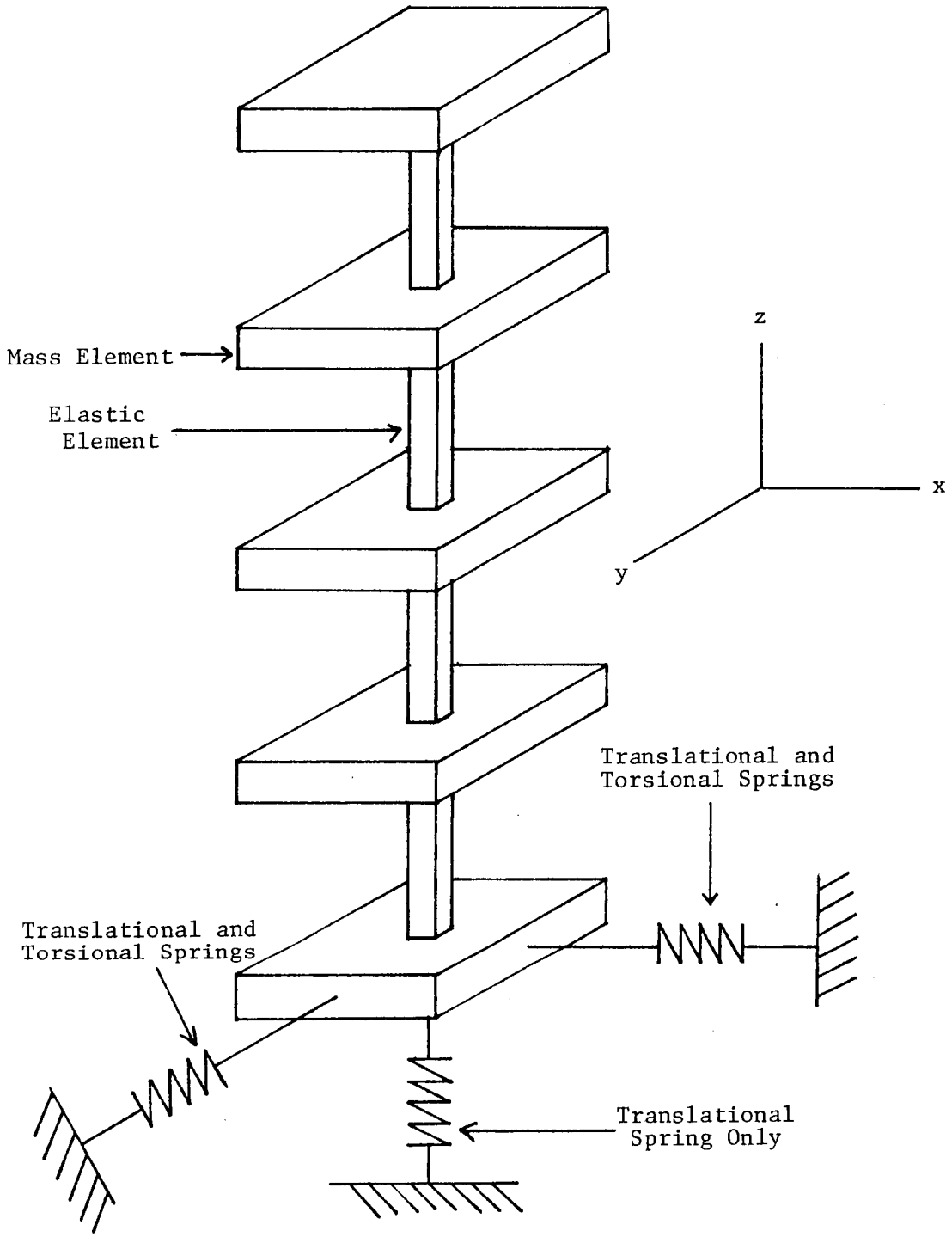


Figure 1. Structural model.

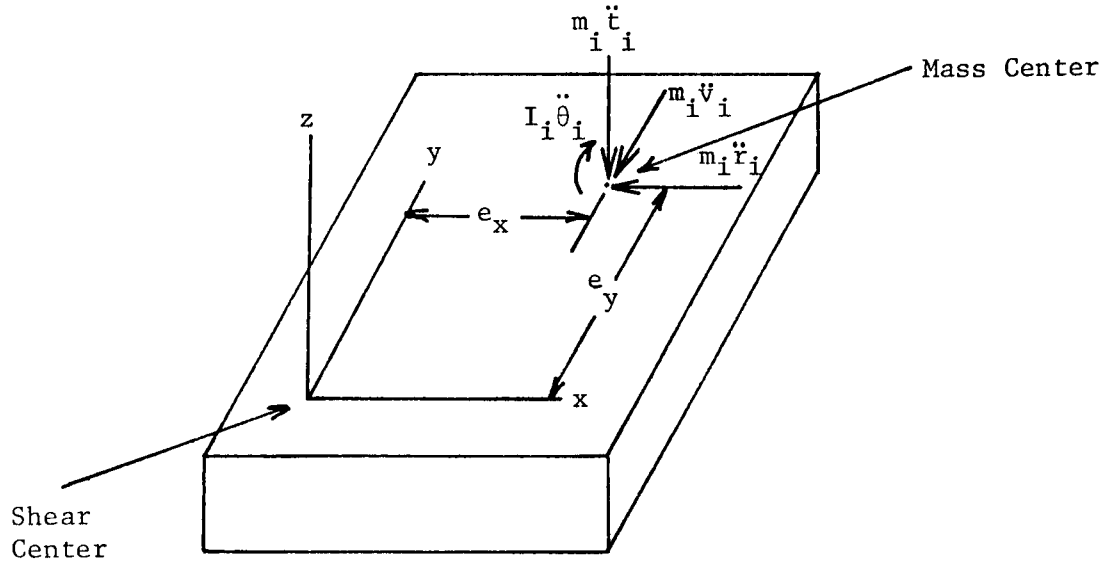


Figure 2. Typical mass element.

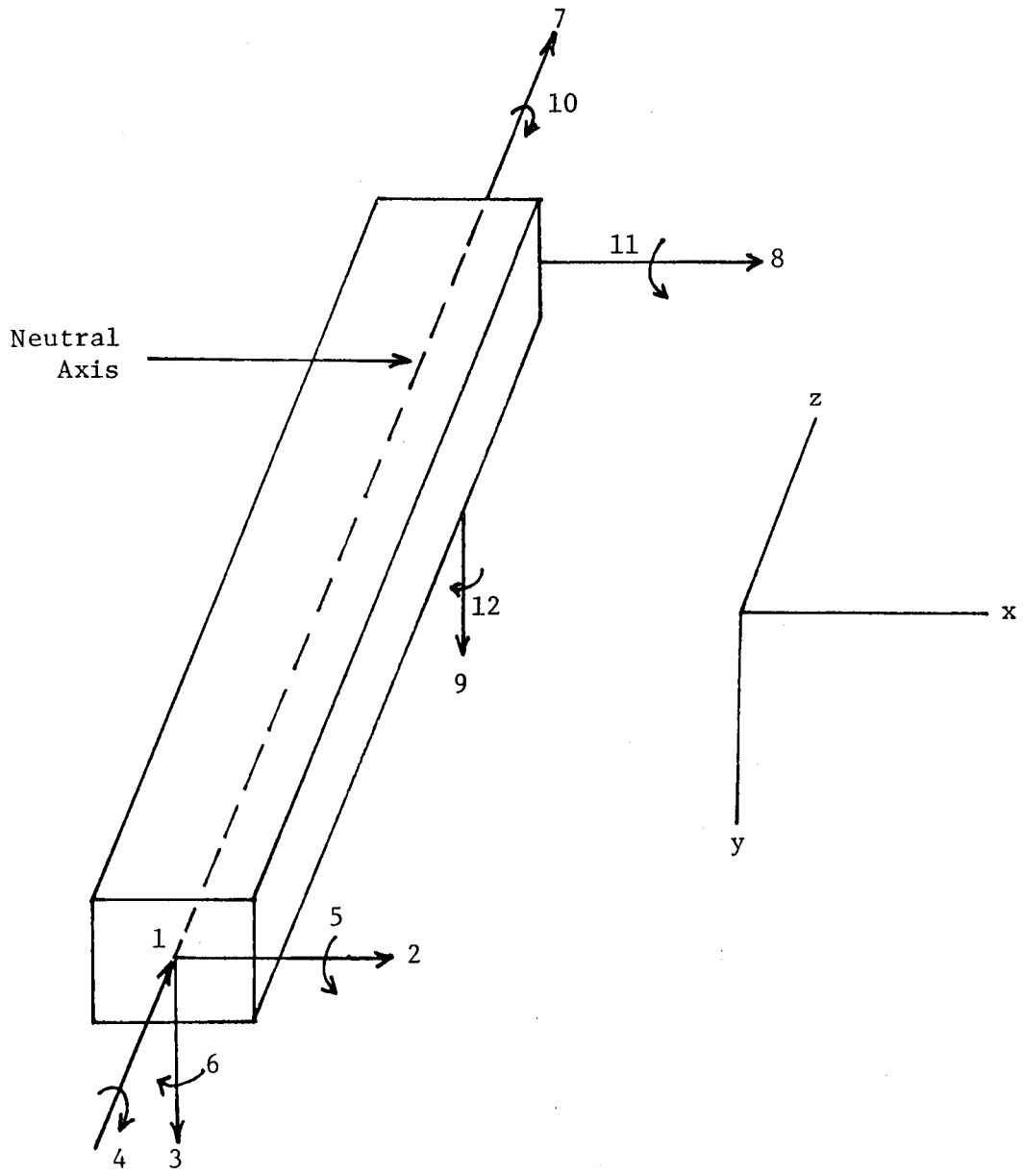


Figure 3. Typical elastic element.

coordinate system depicted in Fig. 4. The coordinates represent mass point displacements.

Equations of Undamped Free Vibration--Lagrange's Equations

Lagrange's equations of motion for a conservative system are

$$\frac{d}{dt}\left(\frac{\partial L}{\partial \dot{q}_i}\right) - \frac{\partial L}{\partial q_i} = 0 \ , \tag{1}$$

where

$L = T - U$,

T = system kinetic energy,

U = system potential energy,

q_i = typical system coordinate,

and the overdot indicates differentiation with respect to time.

The kinetic energy of a typical mass element

$$T_i = \frac{1}{2} m_i\left(\dot{r}_i^2 + \dot{v}_i^2 + \dot{t}_i^2\right) + \frac{1}{2} I_i \dot{\theta}_i^2 \ , \tag{2}$$

where

m_i = mass of the element,

r_i, v_i, t_i = x, y, and z components, respectively, of the mass center displacement,

θ_i = rotation about the z axis (elastic axis) of the element,

I_i = mass moment of inertia of the element about its z axis.

If the base does not move, the kinetic energy of the system is

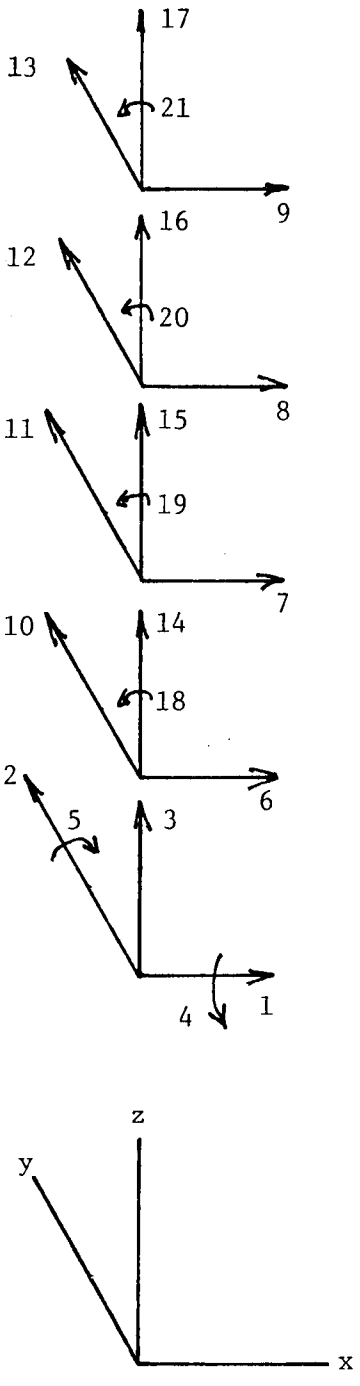


Figure 4. System coordinates.

$$T = \frac{1}{2} \sum_{i=1}^{4} \left[m_i \left(\dot{r}_i^2 + \dot{v}_i^2 + \dot{t}_i^2 \right) + I_i \dot{\theta}_i^2 \right] . \tag{3}$$

If the base moves, the absolute velocity of a typical upper mass element equals its velocity relative to the base plus the base velocity. In this case, the kinetic energy of the system is

$$\begin{aligned} T = {} & \frac{1}{2} m_o \left(\dot{r}_o^2 + \dot{v}_o^2 + \dot{t}_o^2 \right) + \frac{1}{2} I_x^o \dot{\psi}_x^2 + \frac{1}{2} I_y^o \dot{\psi}_y^2 \\ & + \frac{1}{2} \sum_{i=1}^{4} m_i \left[\left(\dot{r}_o + \dot{r}_i + h_i \dot{\psi}_y \right)^2 + \left(\dot{v}_o + \dot{v}_i - h_i \dot{\psi}_x \right)^2 + \left(\dot{t}_o + \dot{t}_i \right)^2 \right] \\ & + \frac{1}{2} \sum_{i=1}^{4} I_x^i \dot{\psi}_x^2 + \frac{1}{2} \sum_{i=1}^{4} I_y^i \dot{\psi}_y^2 + \frac{1}{2} \sum_{i=1}^{4} I_i \dot{\theta}_i^2 , \end{aligned} \tag{4}$$

where

m_o = mass of the base,

r_o, v_o, t_o = x, y, and z components of base displacement,

ψ_x, ψ_y = rotation of the base about its x and y axes,

h_i = height of a typical mass element above the base,

I_x^i, I_y^i = mass moments of inertia of a typical mass element about the x and y axes of the element.

The potential (strain) energy of a typical mass element is

$$\begin{aligned} U_i = {} & \frac{1}{2} \sum_{j=1}^{4} k_{ij}^x s_i s_j + \frac{1}{2} \sum_{j=1}^{4} k_{ij}^y w_i w_j \\ & + \frac{1}{2} \sum_{j=1}^{4} k_{ij}^z t_i t_j + \frac{1}{2} \sum_{j=1}^{4} K_{ij} \theta_i \theta_j , \end{aligned} \tag{5}$$

where

k^x_{ij}, k^y_{ij}, k^z_{ij} = stiffnesses associated with the x, y, and z components of deflection of the elastic axis at the mass element,

s_i, w_i = x and y displacements of the elastic axis at the mass element,

K_{ij} = stiffnesses associated with rotation of the mass element about its z axis.

The mass center and elastic axis displacements are related by the equations

$$r_i = s_i - e_{yi}\theta_i , \tag{6}$$

$$v_i = w_i + e_{xi}\theta_i , \tag{7}$$

where

e_{xi}, e_{yi} = x and y eccentricities of the mass element (see Fig. 2).

If the base does not move, the potential energy of the structure is

$$U = \frac{1}{2}\sum_{i=1}^{4}\sum_{j=1}^{4} k^x_{ij}\left(r_i + e_{yi}\theta_i\right)\left(r_j + e_{yj}\theta_j\right)$$

$$+ \frac{1}{2}\sum_{i=1}^{4}\sum_{j=1}^{4} k^y_{ij}\left(v_i - e_{xi}\theta_i\right)\left(v_j - e_{xj}\theta_j\right)$$

$$+ \frac{1}{2}\sum_{i=1}^{4}\sum_{j=1}^{4} k^z_{ij}t_i t_j + \frac{1}{2}\sum_{i=1}^{4}\sum_{j=1}^{4} K_{ij}\theta_i\theta_j . \tag{8}$$

Including the potential energy associated with base motion, the potential energy of the system is

$$U = \frac{1}{2} K_x r_o^2 + \frac{1}{2} K_y v_o^2 + \frac{1}{2} K_z t_o^2 + \frac{1}{2} G_x \psi_x^2 + \frac{1}{2} G_y \psi_y^2$$

$$+ \frac{1}{2} \sum_{i=1}^{4} \sum_{j=1}^{4} k_{ij}^x \left(r_i + e_{yi}\theta_i\right)\left(r_j + e_{yj}\theta_j\right)$$

$$+ \frac{1}{2} \sum_{i=1}^{4} \sum_{j=1}^{4} k_{ij} \left(v_i - e_{xi}\theta_i\right)\left(v_j - e_{xj}\theta_j\right)$$

$$+ \frac{1}{2} \sum_{i=1}^{4} \sum_{j=1}^{4} k_{ij} t_i t_j + \frac{1}{2} \sum_{i=1}^{4} \sum_{j=1}^{4} K_{ij} \theta_i \theta_j \ , \qquad (9)$$

where

K_x, K_y, K_z, G_x, G_y = stiffnesses associated with deflection of the springs which support the base.

Application of Lagrange's equation yields

$$\ddot{r}_o \left(m_o + \sum_{i=1}^{4} m_i\right) + \ddot{\psi}_y \sum_{i=1}^{4} h_i m_i + \sum_{i=1}^{4} m_i \ddot{r}_i + K_x r_o = 0 \ , \qquad (10)$$

$$\ddot{v}_o \left(m_o + \sum_{i=1}^{4} m_i\right) - \ddot{\psi}_x \sum_{i=1}^{4} h_i m_i + \sum_{i=1}^{4} m_i \ddot{v}_i + K_y v_o = 0 \ , \qquad (11)$$

$$\ddot{t}_o \left(m_o + \sum_{i=1}^{4} m_i\right) + \sum_{i=1}^{4} m_i \ddot{t}_i + K_z t_o = 0 \ , \qquad (12)$$

$$\ddot{\psi}_x \left[I_x^o + \sum_{i=1}^{4} \left(I_x^i + h_i^2 m_i\right)\right] - \ddot{v}_o \sum_{i=1}^{4} h_i m_i - \sum_{i=1}^{4} h_i m_i \ddot{v}_i + \psi_x G_x = 0 \ , \qquad (13)$$

$$\ddot{\Psi}_y \left[I_y^o + \sum_{i=1}^{4} \left(I_y^i + h_i^2 m_i \right) \right] + \ddot{r}_o \sum_{i=1}^{4} h_i m_i + \sum_{i=1}^{4} h_i m_i \ddot{r}_i + \Psi_y G_y = 0 \ , \quad (14)$$

$$\ddot{r}_i m_i + \ddot{r}_o m_i + \ddot{\Psi}_y h_i m_i + \sum_{j=1}^{4} k_{ij}^x \left(r_j + e_{yj} \theta_j \right) = 0 \ , \quad (15)$$

$$\ddot{v}_i m_i + \ddot{v}_o m_i - \ddot{\Psi}_x h_i m_i + \sum_{j=1}^{4} k_{ij}^y \left(v_j - e_{xj} \theta_j \right) = 0 \ , \quad (16)$$

$$\ddot{t}_i m_i + \ddot{t}_o m_i + \sum_{j=1}^{4} k_{ij}^z t_j = 0 \ , \quad (17)$$

$$\ddot{\theta}_i I_i + \sum_{j=1}^{4} \left(k_{ij}^x e_{yi} e_{yj} + k_{ij}^y e_{xi} e_{xj} + K_{ij} \right) \theta_j$$

$$+ \sum_{j=1}^{4} \left(k_{ij}^x e_{yi} r_j - k_{ij}^y e_{xi} v_j \right) = 0 \ . \quad (18)$$

Putting Eqs. (10) through (18) in matrix form, we have

$$[m]\{\ddot{q}\} + [k]\{q\} = \{0\} \ , \quad (19)$$

where

$$\{q\} = \begin{Bmatrix} r_o \\ v_o \\ t_o \\ \Psi_x \\ \Psi_y \\ \{u_1\} \end{Bmatrix} \ ,$$

$$\{u_1\} = \begin{Bmatrix} r_1 \\ r_2 \\ r_3 \\ r_4 \\ v_1 \\ v_2 \\ v_3 \\ v_4 \\ t_1 \\ t_2 \\ t_3 \\ t_4 \\ \theta_1 \\ \theta_2 \\ \theta_3 \\ \theta_4 \end{Bmatrix},$$

[m] is shown in Fig. 5, and [k] is shown in Fig. 6.

The contents of the structural stiffness matrix can be determined from the stiffness properties of the individual elastic elements. The stiffness matrix, $[\kappa]_i$, for a typical element[3] is shown in Fig. 7. The corresponding coordinate system is shown in Fig. 3, p. 5. By definition, $[\kappa]_i$ satisfies

$$\{F\}_i = [\kappa]_i \{\delta\}_i \,, \tag{20}$$

$$[m] = \left[\begin{array}{c|c} [m_{11}] & [m_{12}] \\ \hline [m_{21}] & [m_{22}] \end{array}\right]$$

$$[m_{12}] = \begin{bmatrix} {}^{1}_{4}\{m_i\} & {}^{1}_{4}\{0\} & {}^{1}_{4}\{0\} & {}^{1}_{4}\{0\} \\ {}^{1}_{4}\{0\} & {}^{1}_{4}\{m_i\} & {}^{1}_{4}\{0\} & {}^{1}_{4}\{0\} \\ {}^{1}_{4}\{0\} & {}^{1}_{4}\{0\} & {}^{1}_{4}\{m_i\} & {}^{1}_{4}\{0\} \\ {}^{1}_{4}\{0\} & -{}^{1}_{4}\{m_i h_i\} & {}^{1}_{4}\{0\} & {}^{1}_{4}\{0\} \\ {}^{1}_{4}\{m_i h_i\} & {}^{1}_{4}\{0\} & {}^{1}_{4}\{0\} & {}^{1}_{4}\{0\} \end{bmatrix}$$

$$[m_{21}] = [m_{12}]^T$$

$$[m_{22}] = \begin{bmatrix} \lceil m_i \rfloor & [0] & [0] & [0] \\ [0] & \lceil m_i \rfloor & [0] & [0] \\ [0] & [0] & \lceil m_i \rfloor & [0] \\ [0] & [0] & [0] & \lceil I_i \rfloor \end{bmatrix}$$

$$[m_{11}] = \begin{bmatrix} m_T & 0 & 0 & 0 & m_t \\ 0 & m_T & 0 & -m_t & 0 \\ 0 & 0 & m_T & 0 & 0 \\ 0 & -m_t & 0 & m_{44} & 0 \\ m_t & 0 & 0 & 0 & m_{55} \end{bmatrix}$$

$$m_T = m_o + \sum_{i=1}^{4} m_i$$

$$m_t = \sum_{i=1}^{4} m_i h_i$$

$$m_{44} = I_x^o + \sum_{i=1}^{4} (I_x^i + m_i h_i^2)$$

$$m_{55} = I_y^o + \sum_{i=1}^{4} (I_y^i + m_i h_i^2)$$

Figure 5. Mass matrix.

$$
\begin{bmatrix}
K_x & 0 & 0 & 0 & 0 & & & & \\
0 & K_y & 0 & 0 & 0 & & & & \\
0 & 0 & K_z & 0 & 0 & & \text{ZEROS} & & \\
0 & 0 & 0 & G_x & 0 & & & & \\
0 & 0 & 0 & 0 & G_y & & & & \\
 & & & & & [k^x_{ij}] & [0] & [0] & [k_{14}] \\
 & & \text{ZEROS} & & & [0] & [k^y_{ij}] & [0] & [k_{24}] \\
 & & & & & [0] & [0] & [k^z_{ij}] & [0] \\
 & & & & & [k_{41}] & [k_{42}] & [0] & [k_{44}]
\end{bmatrix}
$$

$$[k_{14}] = [k^x_{ij} e_{yj}]$$

$$[k_{24}] = [-k^y_{ij} e_{xj}]$$

$$[k_{41}] = [k^x_{ij} e_{yi}]$$

$$[k_{42}] = [-k^y_{ij} e_{xi}]$$

$$[k_{44}] = [k^x_{ij} e_{yi} e_{yj} + k^y_{ij} e_{xi} e_{xj} + K_{ij}]$$

All the indicated submatrices are of order 4.

Figure 6. Structural stiffness matrix.

$$
\begin{bmatrix}
\frac{EA}{\ell} & & & & & & & & & & & & \\
0 & \frac{12EI_y}{\ell^3(1+\Phi_x)} & & & & & & & & & & & \\
0 & 0 & \frac{12EI_x}{\ell^3(1+\Phi_y)} & & & & & & & & & & \\
0 & 0 & 0 & \frac{GJ}{\ell} & & & & & & & & & \\
0 & 0 & \frac{-6EI_x}{\ell^2(1+\Phi_y)} & 0 & \frac{(4+\Phi_y)EI_x}{\ell(1+\Phi_y)} & & & & & & & & \\
0 & \frac{6EI_y}{\ell^2(1+\Phi_x)} & 0 & 0 & 0 & \frac{(4+\Phi_x)EI_y}{\ell(1+\Phi_x)} & & & & & & & \\
\frac{-EA}{\ell} & 0 & 0 & 0 & 0 & 0 & \frac{AE}{\ell} & & & & & & \\
0 & \frac{-12EI_y}{\ell^2(1+\Phi_x)} & 0 & 0 & 0 & \frac{-6EI_y}{\ell^2(1+\Phi_x)} & 0 & \frac{12EI_y}{\ell^3(1+\Phi_x)} & & & & & \\
0 & 0 & \frac{-12EI_x}{\ell^2(1+\Phi_y)} & 0 & \frac{6EI_x}{\ell^2(1+\Phi_y)} & 0 & 0 & 0 & \frac{12EI_x}{\ell^3(1+\Phi_y)} & & & & \\
0 & 0 & 0 & \frac{-GJ}{\ell} & 0 & 0 & 0 & 0 & 0 & \frac{GJ}{\ell} & & & \\
0 & 0 & \frac{-6EI_x}{\ell^2(1+\Phi_y)} & 0 & \frac{(2-\Phi_y)EI_x}{\ell(1+\Phi_y)} & 0 & 0 & 0 & \frac{6EI_x}{\ell^2(1+\Phi_y)} & 0 & \frac{(4+\Phi_y)EI_x}{\ell(1+\Phi_y)} & & \\
0 & \frac{6EI_y}{\ell^2(1+\Phi_x)} & 0 & 0 & 0 & \frac{(2-\Phi_x)EI_y}{\ell(1+\Phi_x)} & 0 & \frac{-6EI_y}{\ell^2(1+\Phi_x)} & 0 & 0 & 0 & \frac{(4+\Phi_x)EI_y}{\ell(1+\Phi_x)}
\end{bmatrix}
$$

Symmetric

E = elastic modulus of the element material

G = shear modulus of the element material

A = element cross-sectional area

J = polar area moment of the element cross section

ℓ = element length

Φ_x, Φ_y = shear coefficients

I_x, I_y = second area moment of the element cross section about its x and y axes

Figure 7. Element stiffness matrix.

where

$\{F\}_i$ = vector of applied element forces,

$\{\delta\}_i$ = vector of element displacements.

It can be shown[4] that the structural stiffness matrix, $[K]$, for the four elastic members satisfies

$$[K] = [\beta]^T[\kappa][\beta] \ , \tag{21}$$

where

$$[\kappa] = \begin{bmatrix} [\kappa]_1 & & & 0 \\ & [\kappa]_2 & & \\ & & [\kappa]_3 & \\ 0 & & & [\kappa]_4 \end{bmatrix}$$

$[\beta]$ satisfies

$$\begin{Bmatrix} \{\delta\}_1 \\ \{\delta\}_2 \\ \{\delta\}_3 \\ \{\delta\}_4 \end{Bmatrix} = [\beta]\{u\} \ ,$$

$$\{u\} = \begin{Bmatrix} \{u_1\} \\ \alpha_1 \\ \alpha_2 \\ \alpha_3 \\ \alpha_4 \\ \gamma_1 \\ \gamma_2 \\ \gamma_3 \\ \gamma_4 \end{Bmatrix} \ ,$$

α_i, γ_i = rotation of typical mass element about its x and y axes.

Then

$$\{F\} = [K]\{u\} , \tag{22}$$

where

$\{F\}$ = force vector associated with the displacement vector $\{u\}$.

For the system at hand, we wish to find the matrix [k] of order 21 which satisfies

$$\{F\} = [k]\{q\} , \tag{23}$$

where

$\{F\}$ = force vector associated with the displacement vector $\{q\}$.

The upper left (5 × 5), lower left (16 × 5) and upper right (5 × 16) submatrices of [k] are known. The unknown lower right (16 × 16) submatrix of [k] represents the stiffness of the elastic elements with independent rocking permitted but not included in the equations of motion. That is, the required matrix, $[k_1]$, satisfies

$$\{F_1\} = [k_1]\{u_1\} , \tag{24}$$

where

$\{F_1\}$ = force vector associated with the displacement vector $\{u_1\}$, which is defined in Eq. (19).

The matrix, [K], which is of order 24, can be reduced to $[k_1]$, which is of order 16, by a static condensation.[4]

Eigenvalue Problem

Equation (19) represents a system of 21 coupled equations of undamped free vibration. Since structural response to ground motion is represented by damped forced vibration, Eq. (19) is not a complete statement of the problem at hand. However, the solution of Eq. (19) leads to an eigenvalue problem which can be solved for the natural frequencies (square roots of the eigenvalues) and mode shapes (eigenvectors) of the system.[5] And, for certain kinds of damping, the matrix whose columns are the mode shapes (referred to as the modal matrix) can be used to uncouple the equations of damped forced vibration.

The eigenvalue problem resulting from the solution of Eq. (19) is

$$[k]\{\phi\}_i = \omega_i^2[m]\{\phi\}_i \ , \tag{25}$$

where

$\{\phi\}_i$ = typical mode shape,

ω_i = typical natural frequency.

In general, there are as many mode shapes and frequencies as there are degrees of freedom in the system. The solution of Eq. (19) can be represented by

$$\{q\} = \sum_{i=1}^{21} A_i\{\phi\}_i \cos(\omega_i t - \Psi_i) \ , \tag{26}$$

where

t = time,

A_i, Ψ_i = constants determined by the initial conditions of the motion.

The properties of the mode shapes which are of use in uncoupling the equations of damped forced vibration are

$$[\Phi]^T[k][\Phi] = [K] , \tag{27}$$

$$[\Phi]^T[m][\Phi] = [M] , \tag{28}$$

where

$[\Phi]$ = modal matrix,

$[K]$, $[M]$ = diagonal matrices of stiffness and mass coefficients.

From these equations and Eq. (25), it follows that

$$[K] = [\omega^2][M] , \tag{29}$$

where

$[\omega^2]$ = diagonal matrix of eigenvalues.

Equations of Undamped Vibration with Ground Motion

Thus far, the ground upon which the structure rests has been assumed fixed. With ground translation specified by three orthogonal components, x_g, y_g, and z_g, the system kinetic energy becomes

$$\begin{aligned} T = {} & \frac{1}{2} m_o \left[(\dot{r}_o + \dot{x}_g)^2 + (\dot{v}_o + \dot{y}_g)^2 + (\dot{t}_o + \dot{z}_g)^2 \right] \\ & + \frac{1}{2} \sum_{i=1}^{4} m_i \left[(\dot{x}_g + \dot{r}_o + \dot{r}_i + \dot{\Psi}_y h_i)^2 + (\dot{y}_g + \dot{v}_o + \dot{v}_i - \dot{\Psi}_x h_i)^2 \right. \\ & \left. + (\dot{z}_g + \dot{t}_o + \dot{t}_i)^2 \right] + \frac{1}{2} I^o_x \dot{\Psi}^2_x + \frac{1}{2} I^o_y \dot{\Psi}^2_y \\ & + \frac{1}{2} \sum_{i=1}^{4} (I^i_x \dot{\Psi}^2_x + I^i_y \dot{\Psi}^2_y + I_i \dot{\theta}^2_i) . \end{aligned} \tag{30}$$

With the potential energy given by Eq. (9), the application of Lagrange's equations yields

$$\{P\} + [m]\{\ddot{q}\} + [k]\{q\} = \{0\} \ , \tag{31}$$

where

$$\{P\} = \begin{Bmatrix} m_T \ddot{x}_g \\ m_T \ddot{y}_g \\ m_T \ddot{z}_g \\ -\ddot{y}_g \sum_{i=1}^{4} m_i h_i \\ \ddot{x}_g \sum_{i=1}^{4} m_i h_i \\ m_1 \ddot{x}_g \\ \vdots \\ m_4 \ddot{x}_g \\ m_1 \ddot{y}_g \\ \vdots \\ m_4 \ddot{y}_g \\ m_1 \ddot{z}_g \\ \vdots \\ m_4 \ddot{z}_g \\ 0 \\ 0 \\ 0 \\ 0 \end{Bmatrix} \ ,$$

and

$$m_T = m_o + \sum_{i=1}^{4} m_i \ .$$

In the present case, $\ddot{x}_g$, $\ddot{y}_g$, and $\ddot{z}_g$ are known functions of time representing strong motion of a seismic disturbance. Moving $\{P\}$ to the right hand side of Eq. (31) gives

$$[m]\{\ddot{q}\} + [k]\{q\} = -\{P\} \ . \tag{32}$$

The inertial forces, $\{P\}$, generated by the ground motion now appear as the excitation for the relative motion of the structure, which is represented by the displacements $\{q\}$.

Equations of Damped Vibration with Ground Motion

At this point, damping is introduced into the equations of motion. That is, we include terms which represent internal energy dissipation by the system. Specifically, Eq. (32) becomes

$$[m]\{\ddot{q}\} + [c]\{q\} + [k]\{q\} = -\{P\} \ , \tag{33}$$

where $[c]$ is the damping matrix.

It has been shown[6] that the modal matrix of the undamped system, $[\Phi]$, can be used to uncouple the equations of the damped system, if $[c]$ satisfies

$$[m]^{-1/2}[c][m]^{-1/2} = \sum_{s=1}^{n} \sum_{p=0}^{n-1} \alpha_{sp} \left([m]^{-1/2}[k][m]^{-1/2} \right)_j^{p/s} \ , \tag{34}$$

where

n = number of degrees of freedom,

p, s = integers,

α_{sp} = constants,

and the subscript, j, denotes one particular root of the matrix in parentheses. If we were to use a damping matrix that did not satisfy Eq. (34), the damped equations could still be uncoupled; but the natural frequencies and mode shapes of the damped system would differ from those of the undamped system. The modal matrix for the damped system could then be found only if damping were introduced prior to solving the eigenvalue problem. Furthermore, the resulting eigenvalues and eigenvectors would, in general, be complex. For the sake of simplicity, then, [c] is chosen here to satisfy Eq. (34).

Meirovitch points out that if we choose

$$\alpha_{sp} = 0 \qquad \text{for} \qquad s > 1,\ p > 1\ ,$$

Eq. (34) can be written

$$[c] = \alpha_{10}[m] + \alpha_{11}[k]\ . \tag{35}$$

A damping matrix which satisfies Eq. (35) is said to be proportional.[7] Physically, proportional damping represents one form of viscous damping; and its accuracy as a damping model depends on the structure being modeled. Since no particular structure is being modeled in the present analysis, Eq. (35) is as justifiable as any other form of Eq. (34). Hence, again for simplicity, proportional damping is chosen for the system. The damping will later be specified in terms of modal damping ratios.

Modal Analysis

Equation (33) represents a system of 21 coupled equations of damped forced vibration. To uncouple these equations, first define modal coordinates, $\{\eta\}$, such that

$$\{q\} = [\Phi]\{\eta\} \ . \tag{36}$$

Now substitute into Eq. (33) and premultiply the result by the transpose of the modal matrix to give

$$\begin{aligned} &[\Phi]^T[m][\Phi]\{\ddot{\eta}\} + [\Phi]^T[c][\Phi]\{\eta\} \\ &+ [\Phi]^T[k][\Phi]\{\eta\} = -[\Phi]^T\{P\} \ . \end{aligned} \tag{37}$$

In view of Eqs. (27), (28), (29), and (35), Eq. (37) can be written

$$\begin{aligned} &[M]\{\ddot{\eta}\} + (\alpha_{10}[M] + \alpha_{11}[\omega^2][M])\{\dot{\eta}\} \\ &+ [\omega^2][M]\{\eta\} = -[\Phi]^T\{P\} \ , \end{aligned} \tag{38}$$

which represents a system of 21 uncoupled equations of damped forced vibration. A typical equation from this set is written

$$\begin{aligned} &M_{ii}\ddot{\eta}_i + (\alpha_{10} + \omega_i^2\alpha_{11})M_{ii}\dot{\eta}_i + \omega_i^2 M_{ii}\eta_i \\ &\quad = -m_T(\ddot{x}_g\phi_{1i} + \ddot{y}_g\phi_{2i} + \ddot{z}_g\phi_{3i}) \\ &\quad + (\ddot{y}_g\phi_{4i} - \ddot{x}_g\phi_{5i}) \sum_{j=1}^{4} m_j h_j \\ &\quad - \ddot{x}_g \sum_{j=6}^{9} m_j\phi_{ji} - \ddot{y}_g \sum_{j=10}^{13} m_j\phi_{ji} - \ddot{z}_g \sum_{j=14}^{17} m_j\phi_{ji} \ , \end{aligned} \tag{39}$$

where

M_{ii} = typical mass coefficient,

η_i = typical modal coordinate,

ϕ_{ji} = element j of mode shape i.

This equation can also be written

$$\ddot{\eta}_i + 2\zeta_i\omega_i\dot{\eta}_i + \omega_i^2\eta_i = -\Gamma_i^x\ddot{x}_g - \Gamma_i^y\ddot{y}_g - \Gamma_i^z\ddot{z}_g \,, \tag{40}$$

where

$$\zeta_i = \frac{1}{2}\left(\frac{\alpha_{10}}{\omega_i} + \alpha_{11}\omega_i\right) \,,$$

and the modal participation factors are given by

$$\Gamma_i^x = \frac{1}{M_{ii}}\left(m_T\phi_{1i} + \phi_{5i}\sum_{j=1}^{4} m_j h_j + \sum_{j=6}^{9} m_j\phi_{ji}\right) \,,$$

$$\Gamma_i^y = \frac{1}{M_{ii}}\left(m_T\phi_{2i} - \phi_{4i}\sum_{j=1}^{4} m_j h_j + \sum_{j=10}^{13} m_j\phi_{ji}\right) \,,$$

$$\Gamma_i^z = \frac{1}{M_{ii}}\left(m_T\phi_{3i} + \sum_{j=14}^{17} m_j\phi_{ji}\right) \,.$$

The modal damping ratios, ζ_i, chosen for the present case are discussed in Section IV.

III. SOLUTIONS TO THE PROBLEM

Time History Analysis

Because they are uncoupled, the 21 modal equations represented by Eq. (40) can be solved independently to give $\{\eta\}$ as functions of time. The values of $\{q\}$ at any time can be found from the values of $\{\eta\}$ for that time and Eq. (36). Once the time histories of $\{q\}$ are developed, the maximum values of each of the system coordinates is available by inspection. For purposes of this study, time history analysis was performed for simultaneous application of three spatial components of ground motion. The maximum values of the system coordinates resulting from this analysis were used as a standard for evaluating the various response spectrum analysis techniques discussed below.

Response Spectrum Analysis

Unfortunately, it is not possible to express the ground motion of future seismic disturbances as functions of time. Nor is it prudent to use but one earthquake record for structural design excitation. Rather, a structure should be designed to survive, with little or no damage, all seismic disturbances it is likely to encounter. To this end, the structural designer turns to response spectrum analysis.

By definition, a response spectrum is, for a given damping ratio and excitation, the maximum responses of a family of damped, single degree of freedom oscillators plotted against the natural frequencies of the oscillators. The equation of a damped, single degree of freedom oscillator excited by ground motion is

$$\ddot{u} + 2\zeta\omega\dot{u} + \omega^2 u = -\ddot{s}_g \quad , \tag{41}$$

where

u = relative displacement,

ζ = damping ratio,

ω = natural frequency,

$\ddot{s}_g$ = ground motion specified as a function of time.

To obtain a response spectrum for $\ddot{s}_g$, it is first necessary to choose a value for ζ. Then, for a given value of ω, Eq. (41) is integrated over the time interval for which $\ddot{s}_g$ is specified. The maximum value of u is plotted vs the value of ω. The integration and plotting are repeated for as many values of ω as are of interest. For a given damping ratio, a given excitation has a unique response spectrum. But any number of excitations can produce the same response spectrum.

Through comparison of response spectra of past earthquakes and consideration of geological data, it is possible to produce a design response spectrum for a given site, i.e., a response spectrum representing the maximum structural amplification of a specified level of ground excitation. It is a design response spectrum, then, and not a time history of ground motion, with which the structural designer must work.

Given the modal analysis of a structure, and a design response spectrum for a site, one cannot compute the maximum structural response. In order to compute structural response, $\{q\}$, at a given time, one requires the values of all modal coordinates, $\{\eta\}$, for that time. The

response spectrum provides only the maximum values of the modal coordinates. That is,

$$(\eta_i^s)_{max} = \Gamma_i^s \, (u_i^s)_{max} \, , \tag{42}$$

where

$(\eta_i^s)_{max}$ = maximum value of typical modal coordinate in response to $\ddot{s}_g$,

Γ_i^s = typical modal participation factor,

$(u_i^s)_{max}$ = value from response spectrum for ω equal to ω_i.

In general, these maxima do not all occur at the same time. In fact, the response spectrum reveals nothing about when the maxima occur, nor about the values of the other modal coordinates when any one of the maxima occurs. Therefore, response spectrum analysis does not yield the values of $\{q\}$ for any time.

Although the maximum system response cannot be calculated precisely from response spectrum analysis, it can be approximated. As indicated in the section on modal analysis, the system and modal coordinates are related by Eq. (36). If the $\{\eta\}$ were all known for one instant of time, we could find a typical system coordinate for that time by

$$q_i = \sum_{j=1}^{21} \phi_{ij} \eta_j \, . \tag{43}$$

But from response spectrum analysis, we have only the maximum modal coordinate values given by

$$\{\eta^x\}_{max} = \{\Gamma^x u^x_{max}\} \ , \tag{44}$$

$$\{\eta^y\}_{max} = \{\Gamma^y u^y_{max}\} \ , \tag{45}$$

$$\{\eta^z\}_{max} = \{\Gamma^z u^z_{max}\} \ , \tag{46}$$

where the $\{u\}$ are response spectrum values, and the superscripts indicate the spatial component of the ground motion. Since the $\{\eta\}_{max}$ are not functionally related to the $\{q\}_{max}$, it is desired to find an equation similar to Eq. (43) that approximates the $\{q\}_{max}$ in terms of the ϕ_{ij} and the $\{\eta\}_{max}$. The equations discussed below were all evaluated for this study. The response spectra used were generated from the three spatial components of ground motion used in the time history analysis.

Absolute sum.[1] In this method, the absolute values of the modal responses are added. That is,

$$(q_i^s)_{max} = \sum_{j=1}^{21} |\phi_{ij}(\eta_i^s)_{max}| \ , \tag{47}$$

where the superscript refers to the component of excitation considered. This equation implies that all the modal maxima occur at once, and represents an upper bound for $(q_i^s)_{max}$. After applying Eq. (47) for each of the three components of excitation, the results are combined by

$$(q_i)_{max} = \left[(q_i^x)^2_{max} + (q_i^y)^2_{max} + (q_i^z)^2_{max}\right]^{1/2} \ . \tag{48}$$

Square root of sum of squares.[8] As is clear from its name, the equation is

$$(q_i^s)_{max} = \left\{ \sum_{j=1}^{21} \left[\phi_{ij} (\eta_j^s)_{max} \right]^2 \right\}^{1/2} . \tag{49}$$

As in the absolute sum method, Eq. (48) is used to combine the results for the three components of ground motion.

Double sum.[9] This method attempts to take into account the mutual reinforcement that occurs between two modes if their natural frequencies are nearly equal. The equation is

$$(q_i^s)_{max} = \left[\sum_{j=1}^{21} \sum_{k=1}^{21} \phi_{ij} (\eta_j^s)_{max} \phi_{ik} (\eta_k^s)_{max} \varepsilon_{jk} \right]^{1/2} , \tag{50}$$

where

$$\varepsilon_{jk} = \left[1 + \left(\frac{\omega_j' - \omega_k'}{\beta_j \omega_j + \beta_k \omega_k} \right)^2 \right]^{-1} ,$$

$$\omega_j' = \omega_j \left(1 - \beta_j^2 \right)^{1/2} ,$$

$$\beta_j = \zeta_j + \frac{2}{t_d \omega_j} ,$$

t_d = duration of ground motion.

Note that Eq. (49) is a special case of Eq. (50) with

$$\varepsilon_{jk} = 0 \qquad \text{for} \qquad j \neq k .$$

As in the previous methods, Eq. (48) is used to combine the results from the three ground motion components.

Closely spaced modes.[10] Like the double sum method, this method attempts to account for intermodal coupling. But rather than include

all the cross products and calculate a coupling coefficient for each one, this method mixes the first two methods. For modes in a closely spaced group, the absolute sum method is first applied. Then, the square root of the sum of the squares method is applied to the group totals and the remaining well-separated modes. A closely spaced group includes those modes whose frequencies lie between the lowest in the group and a frequency 10% higher. The equation is

$$(q_i^s)_{max} = \left\{ \sum_{j=1}^{k} \left[\phi_{ij} (\eta_j^s)_{max} \right]^2 + \sum_{\ell=1}^{m} \left[\sum_{n=1}^{p_\ell} \left| \phi_{in} (\eta_n^s)_{max} \right| \right]^2 \right\}^{1/2} , \qquad (51)$$

where

$k = 21 - \sum_{\ell=1}^{m} p_\ell$, number of well-separated modes,

m = number of groups of closely spaced modes,

p_ℓ = number of modes in group ℓ.

Note that the subscripts j and n do not indicate the positions of ϕ_{ij} and ϕ_{in} in the mode shape vectors. These positions are determined by the relative magnitudes of the modal frequencies of the model being used. Equation (48) is applied as before.

Lin's method. (After Lin.[2]) Lin's method differs significantly from the others discussed here. Rather than compute the maximum system response to each component of ground motion by absolute sums and then combine by the square root of the sum of the squares, this method first combines absolutely the modal maxima due to the three components of excitation and then computes the overall maximum system response by taking the square root of the sum of the squares. The equation is

$$(q_i)_{max} = \left(\sum_{j=1}^{21} \left\{ \phi_{ij} \left[\left| (\eta_j^x)_{max} \right| + \left| (\eta_j^y)_{max} \right| + \left| (\eta_j^z)_{max} \right| \right] \right\}^2 \right)^{1/2} . \qquad (52)$$

IV. NUMERICAL DATA AND PROCEDURES

Structural Data

The inertial and stiffness data for the structural model are presented in Tables 1, 2, and 3. The moments of inertia of the upper floors about their horizontal axes are neglected. The data exhibit much symmetry, which suggests a rather regular structure. While the model contains the dynamic parameters needed to model a more irregular structure, the choice of a fairly uniform structure insures that closely spaced modes will occur.

Eigenvalue Problem

Assembly of the structural mass and stiffness matrices and solution of the eigenvalue problem were accomplished by a FØRTRAN computer program developed for the model and made available by Dr. T. G. Carley, Associate Professor of Engineering Science and Mechanics, the University of Tennessee, Knoxville. The program first transforms Eq. (25) into the standard form of the eigenvalue problem

$$[P]\{z\}_i = \omega_i^2\{z\}_i \ , \tag{53}$$

where

$\{z\}_i$ = typical eigenvector of [P],

$[P] = [L]^{-1}[k][L]^{-1^T}$,

[L] = lower triangular Choleski decomposition matrix of [m].

After putting [P] into tridiagonal form, the program uses the Sturm sequence of the matrix, in conjunction with an iterative bisection technique, to compute the eigenvalues and eigenvectors. The

TABLE 1. STRUCTURAL MASS DATA

Mass Point	Mass (slugs)	I_x^i (slug-ft^2)	I_y^i (slug-ft^2)	I_i (slug-ft^2)
Base	73.72	5717	5715	——
1	74.28	0	0	1.689×10^5
2	74.28	0	0	1.689×10^5
3	74.28	0	0	1.689×10^5
4	37.14	0	0	8.539×10^4

TABLE 2. STIFFNESS DATA FOR ELASTIC ELEMENTS

Element	
ℓ (ft)	10
A (ft^2)	185.4
E (psi)	1.44×10^5
E/G	2.5
Φ_x, Φ_y	4.444
I_x, I_y (ft^4)	1.6264×10^5
J (ft^4)	2.934×10^5

TABLE 3. STIFFNESS DATA FOR BASE SPRINGS

K_x (lb/ft)	K_y (lb/ft)	K_z (lb/ft)	G_x (ft-lb/rad)	G_y (ft-lb/rad)
1.0×10^6	1.0×10^6	1.0×10^6	1.0×10^{10}	1.0×10^{10}

eigenvectors, $\{z\}_i$, are then transformed back into the $\{\phi\}_i$ of the original problem.

Excitation

The ground motion components used for this study were provided by Dr. T. G. Carley, Associate Professor of Engineering Science and Mechanics, the University of Tennessee, Knoxville. They are artificial earthquake records (ground acceleration given numerically at 0.01 second intervals) generated by a spectrum modification technique from response spectra compatible with U.S. NRC Regulatory Guide 1.60. These spectra were originally computed from recorded accelerograms of the 1934 El Centro earthquake ($\ddot{x}_g$), the 1940 El Centro earthquake ($\ddot{y}_g$), and the 1939 Olympia earthquake ($\ddot{z}_g$), all using a modal damping ratio of 0.05. The excitation duration is 20 seconds.

Time History Analysis

The time history analysis was performed by a FØRTRAN computer program (MSESM) listed in the Appendix. The program simultaneously integrates all 21 modal equations [see Eq. (40)], stopping at intervals of 0.05 seconds to convert to system coordinates. The program prints the maximum values obtained by each of the system displacements. MSESM performs numerical integration using a fourth order Runge-Kutta technique. The equations for a typical time interval are

$$\eta_{n+1} = \eta_n + h\dot{\eta}_i + \frac{h}{6}(k_1 + k_2 + k_3) \ , \tag{54}$$

$$\dot{\eta}_{n+1} = \dot{\eta}_n + \frac{1}{6}(k_1 + 2k_2 + 2k_3 + k_4) \ , \tag{55}$$

where

$$k_1 = h\, f(t_n, \eta_n, \dot{\eta}_n) \ ,$$

$$k_2 = h\, f\left(t_n + \frac{h}{2} \ , \ \eta_n + \frac{h}{2}\dot{\eta}_n \ , \ \dot{\eta}_n + \frac{k_1}{2}\right) \ ,$$

$$k_3 = h\, f\left(t_n + \frac{h}{2} \ , \ \eta_n + \frac{h}{2}\dot{\eta}_n + \frac{h}{4}k_1 \ , \ \dot{\eta}_n + \frac{k_2}{2}\right) \ ,$$

$$k_4 = h\, f(t_n + h, \ \eta_n + h\dot{\eta}_n + \frac{h}{2}k_2 \ , \ \dot{\eta}_n + k_3) \ ,$$

h = integration time step,

t = time,

$$f(t, \eta, \dot{\eta}) = -2\zeta_i\omega_i\dot{\eta}_i - \omega_i^2\eta_i - \Gamma_i^x\ddot{x}_g - \Gamma_i^y\ddot{y}_g - \Gamma_i^z\ddot{z}_g \ .$$

The integration time step was one-tenth of the period of the particular equation being integrated; i.e., a different time step was used for each modal equation. The modal damping ratio was 0.05 for all modes.

Response Spectrum Analysis

Spectral values, $(u_i^s)_{max}$, for each of the three components of ground motion were generated by the method discussed on page 26. The integration was performed only for values of ω equal to the natural frequencies of the system modes. Again, the integration was performed by MSESM with an integration time step of one-tenth the period of the equation being integrated and with a modal damping ratio of 0.05 for all modes. For this case,

$$f(t, \eta, \dot{\eta}) = -2\zeta_i\omega_i\dot{\eta}_i - \omega_i^2\eta_i - \ddot{s}_g \ , \tag{56}$$

where

s = x, y, or z.

V. RESULTS AND CONCLUSIONS

Eigenvalue Problem

The natural frequencies, modal participation factors, and mode shapes, as calculated by QUAKE, are presented in Tables 4 through 11. Each mode shape has been normalized with respect to its largest element. As one would expect for such a regular structure, there are several closely spaced modes and several groups of very similar mode shapes; e.g., modes one and two are nearly the same shape except for the signs of the x-coordinates and the greater amount of twisting in mode one.

Several of the mode shapes represent easily identifiable motions. Comparison of the relative signs of the lateral displacements reveals that the first three modes represent rocking of the structure with varying amounts of twisting. In mode three, the twisting is quite strong, indicating that the eccentric masses used in the model cause significant coupling. Such strong torsion also appears in mode 16. Rocking does not occur again until modes 20 and 21.

Modes 4, 14, 17, 18, and 19 represent essentially vertical motion. Since the vertical displacements are not coupled with other displacements in the system, these modes are the only ones in which appreciable vertical motion appears.

Response Spectrum Generation

Plots of the response spectra generated for the three components of ground motion are presented in Figs. 8, 9, and 10. Only the spectral values, $(u_i^s)_{max}$, for the first 19 modes were used in these plots. The

TABLE 4. NATURAL FREQUENCIES AND MODAL PARTICIPATION FACTORS

MODE	NATURAL FREQUENCY	GAMMA X	GAMMA Y	GAMMA Z
1	20.4	-0.542D 00	0.615D 00	-0.306D-22
2	20.5	0.544D 00	0.616D 00	-0.308D-22
3	39.5	-0.116D-02	0.120D-02	-0.639D-21
4	45.7	0.461D-17	0.106D-16	0.671D 00
5	58.6	-0.234D 00	0.305D 00	0.642D-17
6	58.8	-0.237D 00	-0.307D 00	-0.465D-17
7	91.0	-0.220D 00	0.106D 00	-0.501D-16
8	91.4	-0.224D 00	-0.106D 00	0.252D-16
9	109.8	-0.181D 00	0.622D-01	-0.354D-16
10	110.4	-0.177D 00	-0.592D-01	-0.502D-16
11	112.4	0.678D-02	-0.473D-02	0.874D-17
12	133.5	0.738D 00	-0.461D 00	0.570D-15
13	133.5	-0.741D 00	-0.466D 00	0.539D-15
14	149.3	-0.225D-15	-0.180D-14	-0.474D 00
15	168.4	0.123D-01	0.215D-02	0.411D-16
16	198.6	0.512D-02	0.178D-03	0.218D-16
17	252.1	-0.193D-15	0.238D-15	-0.149D 00
18	331.2	0.465D-15	-0.245D-15	-0.508D-01
19	373.7	-0.185D-16	-0.332D-15	-0.102D-01
20	1328.5	-0.157D 01	-0.251D-04	0.416D-14
21	1328.5	0.157D 01	-0.242D-04	-0.292D-14

TABLE 5. MODE SHAPES 1 - 3

DISPLACEMENT COORDINATE	MODE 1	MODE 2	MODE 3
r_0	-0.887D-01	0.895D-01	-0.612D 00
v_0	0.887D-01	0.895D-01	0.612D 00
t_0	-0.416D-25	-0.450D-25	-0.136D-18
Ψ_x	-0.223D-03	-0.225D-03	-0.133D-02
Ψ_y	-0.223D-03	0.225D-03	-0.133D-02
r_1	-0.294D-01	0.299D-01	-0.252D 00
r_2	-0.685D 00	0.685D 00	-0.672D 00
r_3	-0.907D 00	0.907D 00	-0.848D 00
r_4	-0.100D 01	0.100D 01	-0.100D 01
v_1	0.368D 00	0.368D 00	0.418D 00
v_2	0.685D 00	0.685D 00	0.672D 00
v_3	0.907D 00	0.907D 00	0.848D 00
v_4	0.100D 01	0.100D 01	0.100D 01
t_1	-0.142D-21	-0.143D-21	-0.173D-17
t_2	-0.519D-24	-0.693D-24	-0.278D-18
t_3	-0.579D-25	-0.741D-25	-0.130D-18
t_4	-0.914D-25	-0.988D-25	-0.140D-18
θ_1	0.683D-03	-0.176D-17	-0.375D 00
θ_2	0.125D-02	-0.259D-17	-0.694D 00
θ_3	0.164D-02	-0.341D-17	-0.907D 00
θ_4	0.177D-02	-0.370D-17	-0.983D 00

TABLE 6. MODE SHAPES 4 - 6

DISPLACEMENT COORDINATE	MODE 4	MODE 5	MODE 6
r_0	0.194D-16	-0.190D 00	-0.192D 00
v_0	0.121D-15	0.190D 00	-0.192D 00
t_0	0.100D 01	-0.179D-17	0.185D-17
Ψ_x	-0.643D-18	0.205D-03	-0.206D-03
Ψ_y	0.822D-18	0.205D-03	0.206D-03
r_1	0.303D-18	-0.415D 00	-0.418D 00
r_2	-0.451D-16	-0.324D 00	-0.321D 00
r_3	-0.279D-16	0.506D 00	0.507D 00
r_4	-0.718D-16	0.100D 01	0.100D 01
v_1	-0.154D-15	0.589D 00	-0.587D 00
v_2	-0.940D-16	0.324D 00	-0.321D 00
v_3	-0.179D-15	-0.506D 00	0.507D 00
v_4	-0.129D-15	-0.100D 01	0.100D 01
t_1	0.317D 00	0.251D-16	-0.205D-16
t_2	0.557D 00	0.497D-18	-0.115D-17
t_3	0.708D 00	-0.141D-17	0.150D-17
t_4	0.759D 00	-0.861D-18	0.989D-18
θ_1	0.116D-17	0.133D-02	-0.380D-16
θ_2	0.167D-18	0.106D-02	-0.241D-16
θ_3	-0.142D-17	-0.327D-03	0.181D-16
θ_4	0.153D-17	-0.113D-02	0.401D-16

TABLE 7. MODE SHAPES 7 - 9

DISPLACEMENT COORDINATE	MODE 7	MODE 8	MODE 9
r_0	-0.283D 00	-0.285D 00	-0.172D 00
v_0	0.283D 00	-0.285D 00	0.172D 00
t_0	0.646D-16	-0.729D-16	0.172D-15
Ψ_x	-0.127D-03	0.128D-03	0.219D-03
Ψ_y	-0.127D-03	-0.128D-03	0.219D-03
r_1	-0.967D 00	-0.968D 00	-0.424D 00
r_2	0.100D 01	0.100D 01	0.733D 00
r_3	0.602D 00	0.601D 00	-0.612D 00
r_4	-0.625D 00	-0.620D 00	0.100D 01
v_1	0.468D 00	-0.459D 00	0.561D-01
v_2	-0.100D 01	0.100D 01	-0.733D 00
v_3	-0.602D 00	0.601D 00	0.612D 00
v_4	0.625D 00	-0.620D 00	-0.100D 01
t_1	-0.165D-16	0.875D-17	-0.889D-16
t_2	-0.847D-16	0.562D-16	-0.235D-15
t_3	-0.262D-15	0.248D-15	-0.401D-15
t_4	-0.292D-15	0.247D-15	-0.318D-15
θ_1	0.982D-03	-0.348D-16	-0.313D-02
θ_2	-0.153D-02	0.129D-17	-0.373D-02
θ_3	-0.238D-03	0.238D-17	0.304D-02
θ_4	0.237D-02	-0.199D-16	0.215D-02

TABLE 8. MODE SHAPES 10 - 12

DISPLACEMENT COORDINATE	MODE 10	MODE 11	MODE 12
r_0	-0.167D 00	0.311D 00	0.766D 00
v_0	-0.167D 00	-0.311D 00	-0.766D 00
t_0	-0.531D-16	-0.391D-15	0.822D-15
Ψ_x	-0.217D-03	-0.121D-03	-0.175D-03
Ψ_y	0.217D-03	-0.121D-03	-0.175D-03
r_1	-0.430D 00	-0.338D 00	-0.652D 00
r_2	0.745D 00	0.406D 00	-0.693D 00
r_3	-0.634D 00	-0.100D 01	-0.785D 00
r_4	0.100D 01	0.398D-01	-0.739D 00
v_1	-0.625D-01	0.482D 00	0.100D 01
v_2	0.745D 00	-0.406D 00	0.693D 00
v_3	-0.634D 00	0.100D 01	0.785D 00
v_4	0.100D 01	-0.398D-01	0.739D 00
t_1	-0.374D-16	-0.547D-15	-0.183D-15
t_2	0.175D-17	0.133D-14	-0.697D-15
t_3	0.991D-16	0.108D-14	-0.131D-14
t_4	0.382D-16	0.102D-14	-0.156D-14
θ_1	0.762D-15	0.114D 00	-0.212D-03
θ_2	0.863D-15	0.852D-01	-0.187D-02
θ_3	-0.680D-15	-0.449D-01	0.277D-03
θ_4	-0.597D-15	-0.123D 00	0.175D-02

TABLE 9. MODE SHAPES 13 - 15

DISPLACEMENT COORDINATE	MODE 13	MODE 14	MODE 15
r_0	-0.763D 00	-0.166D-15	-0.185D 00
v_0	-0.763D 00	-0.154D-14	0.185D 00
t_0	0.984D-15	-0.499D 00	0.195D-14
ψ_x	-0.177D-03	-0.375D-17	0.191D-03
ψ_y	0.177D-03	0.126D-17	0.191D-03
r_1	0.661D 00	0.189D-15	0.100D 01
r_2	0.684D 00	0.145D-15	0.283D-01
r_3	0.784D 00	0.613D-16	0.977D-01
r_4	0.739D 00	0.212D-15	0.383D 00
v_1	0.100D 01	0.208D-14	-0.410D 00
v_2	0.684D 00	0.119D-14	-0.283D-01
v_3	0.784D 00	0.153D-14	-0.977D-01
v_4	0.739D 00	0.136D-14	-0.383D 00
t_1	-0.335D-15	0.120D 00	0.231D-14
t_2	-0.905D-15	0.475D 00	-0.574D-15
t_3	-0.159D-14	0.845D 00	-0.441D-14
t_4	-0.184D-14	0.100D 01	-0.885D-14
θ_1	0.711D-15	0.662D-17	0.866D-01
θ_2	0.652D-14	-0.730D-17	-0.654D-01
θ_3	-0.973D-15	-0.558D-17	-0.370D-01
θ_4	-0.609D-14	0.149D-16	0.936D-01

TABLE 10. MODE SHAPES 16 - 18

DISPLACEMENT COORDINATE	MODE 16	MODE 17	MODE 18
r_0	-0.748D-01	-0.443D-16	0.528D-17
v_0	0.748D-01	0.160D-15	-0.157D-15
t_0	0.693D-14	-0.479D 00	-0.376D 00
Ψ_x	-0.250D-03	-0.163D-17	-0.246D-16
Ψ_y	-0.250D-03	-0.908D-17	0.424D-16
r_1	0.100D 01	0.505D-16	-0.164D-16
r_2	-0.211D 00	0.189D-15	-0.827D-15
r_3	0.453D 00	0.389D-15	-0.131D-14
r_4	-0.304D 00	0.332D-15	-0.168D-14
v_1	-0.241D 00	-0.141D-15	-0.216D-15
v_2	0.211D 00	-0.227D-15	-0.401D-15
v_3	-0.453D 00	-0.149D-15	-0.428D-15
v_4	0.304D 00	-0.341D-15	-0.884D-15
t_1	-0.137D-13	0.661D 00	0.997D 00
t_2	-0.144D-13	0.100D 01	0.970D-01
t_3	-0.502D-14	0.417D 00	0.471D-01
t_4	0.103D-13	-0.565D-01	0.100D 01
θ_1	0.687D-01	-0.595D-17	0.435D-17
θ_2	-0.126D 00	-0.133D-16	0.463D-17
θ_3	0.163D 00	0.303D-16	-0.357D-17
θ_4	-0.173D 00	-0.321D-16	-0.345D-17

TABLE 11. MODE SHAPES 19 - 21

DISPLACEMENT COORDINATE	MODE 19	MODE 20	MODE 21
r_0	-0.110D-15	-0.453D-03	0.453D-03
v_0	-0.813D-15	-0.453D-03	-0.453D-03
t_0	-0.183D 00	-0.106D-14	-0.400D-15
Ψ_x	-0.165D-16	0.250D-01	0.250D-01
Ψ_y	0.144D-16	-0.250D-01	0.250D-01
r_1	0.137D-16	0.580D-02	-0.580D-02
r_2	-0.836D-16	0.500D 00	-0.500D 00
r_3	-0.395D-15	0.750D 00	-0.750D 00
r_4	-0.445D-15	0.100D 01	-0.100D 01
v_1	0.115D-14	0.250D 00	0.250D 00
v_2	0.820D-16	0.500D 00	0.500D 00
v_3	0.189D-15	0.750D 00	0.750D 00
v_4	0.665D-15	0.100D 01	0.100D 01
t_1	0.638D 00	0.239D-14	0.742D-17
t_2	-0.491D 00	0.545D-16	0.952D-15
t_3	0.100D 01	0.130D-14	0.543D-15
t_4	-0.683D 00	0.333D-14	-0.320D-15
θ_1	0.469D-17	0.913D-14	-0.938D-07
θ_2	0.527D-17	0.573D-14	-0.588D-07
θ_3	0.285D-16	0.137D-15	-0.146D-08
θ_4	-0.631D-16	0.348D-12	-0.358D-05

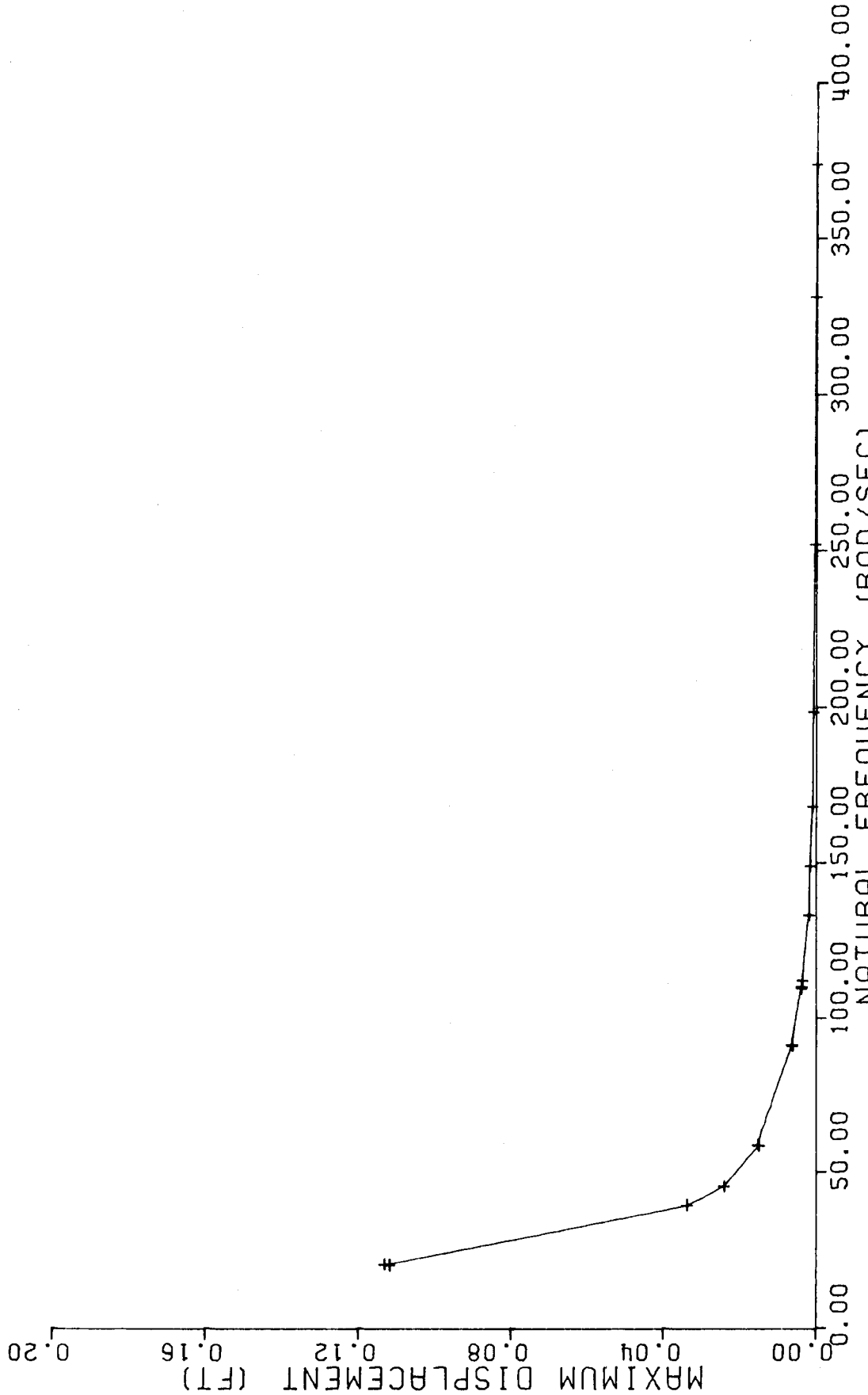


Figure 8. Response spectrum for $\ddot{x}_g$.

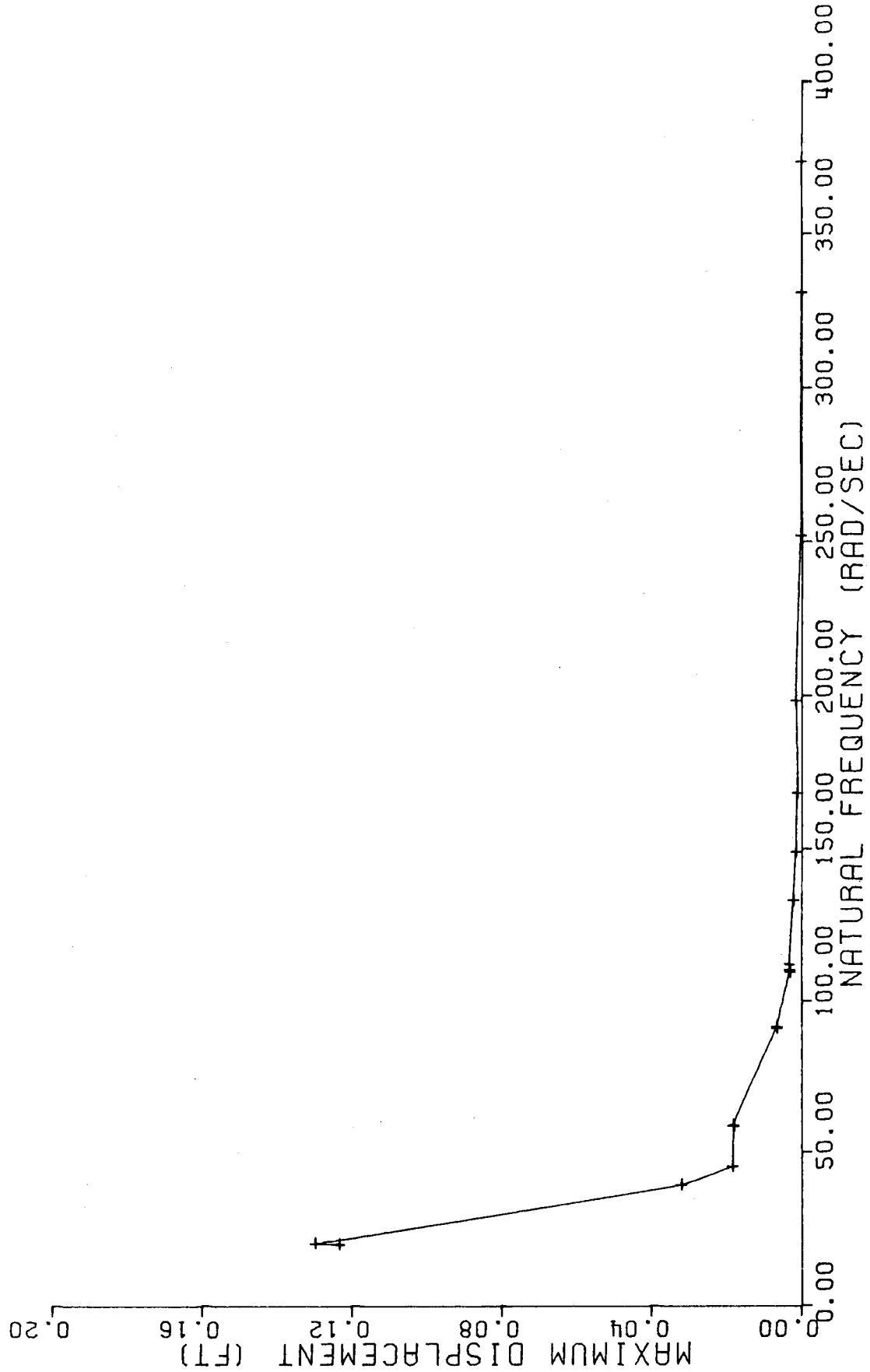


Figure 9. Response spectrum for $\ddot{y}_g$.

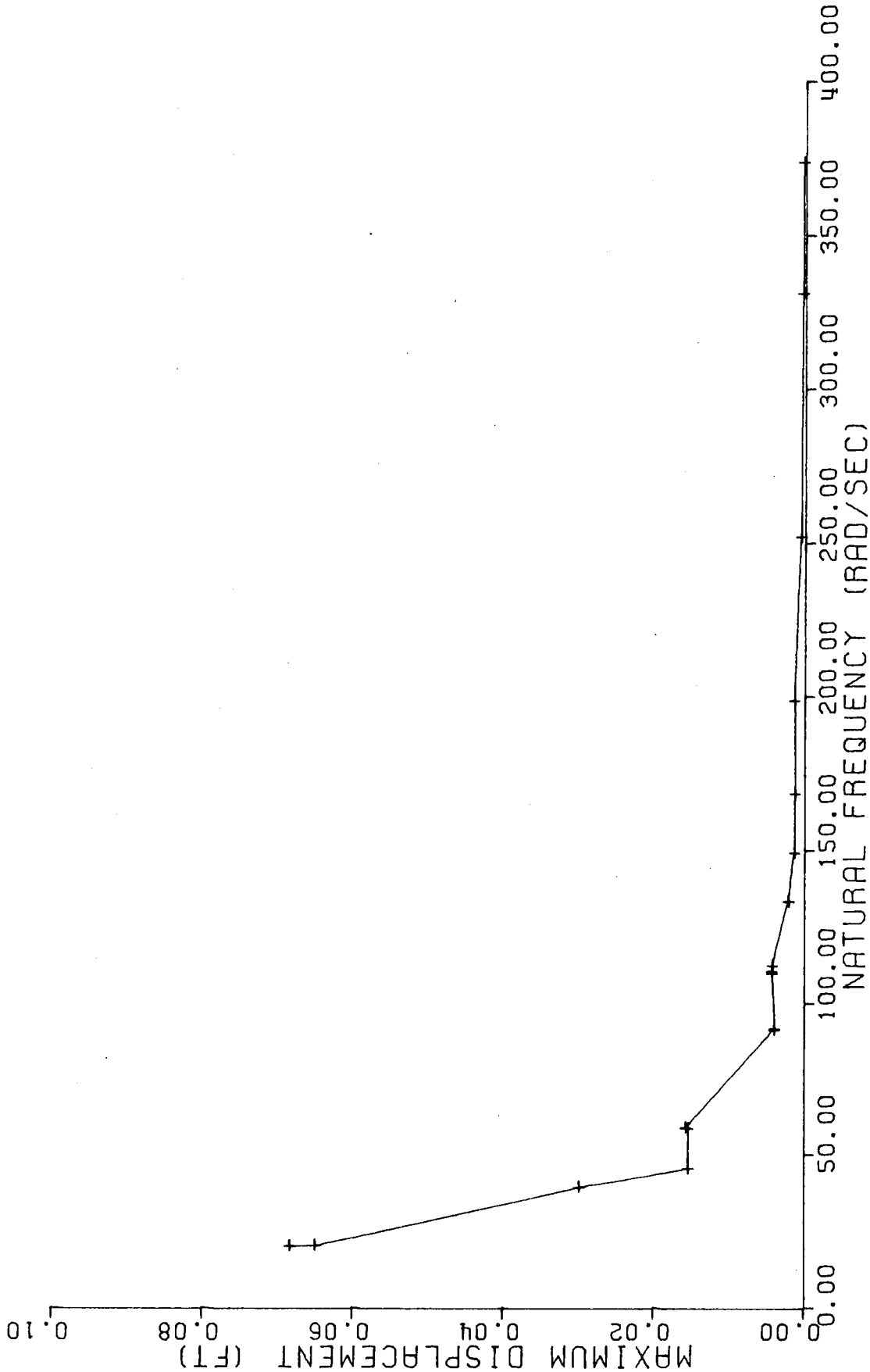


Figure 10. Response spectrum for $\ddot{z}_g$.

frequency content of seismic excitation is typically confined to the range of zero to 35 Hz. Since the modal frequencies for modes 20 and 21 are about 210 Hz, their spectral values are negligible.

Comparison of Response Spectrum Methods

The vectors of maximum system displacements as computed by the time history analysis and the five response spectrum analysis methods, are presented in Tables 12 through 16. A noticeable feature of these results is that in going down the displacement vector, the pattern of variation of the absolute value of the percentage error is roughly the same for all methods. Since the various response spectrum methods are simply different ways of combining the same numbers, this is not surprising. The high percentage errors for system displacement r_1 serve to emphasize the fact that system coordinate maxima are not functionally related to modal coordinate maxima. For any combination of structural model and excitation, one can expect to find certain displacements for which response spectrum analysis does not give good approximations. That all the response spectrum methods gave their worst results for the r_1 displacement simply marks this coordinate as a "difficult" one for the structural model and excitation used in this study. Likewise, the typically low percentage errors in the approximations of the vertical coordinates show that response spectrum analysis can give quite good results for some coordinates.

The vector of maximum displacements from the time history analysis indicates that the structural amplification of the ground motion increases going up the model, and that twisting and vertical motion are

TABLE 12. ABSOLUTE SUM RESULTS

DISPLACEMENT COORDINATE	TIME HISTORY	ESTIMATE	PERCENT ERROR
r_0	0.1096D-01	0.2378D-01	117.02
v_0	0.1430D-01	0.2378D-01	66.34
t_0	0.1044D-01	0.1069D-01	2.41
Ψ_x	0.3547D-04	0.4828D-04	36.10
Ψ_y	0.2765D-04	0.4828D-04	74.59
r_1	0.4129D-02	0.1690D-01	309.35
r_2	0.8327D-01	0.1461D 00	75.39
r_3	0.1118D 00	0.1914D 00	71.28
r_4	0.1240D 00	0.2167D 00	74.70
v_1	0.5755D-01	0.8533D-01	48.28
v_2	0.1076D 00	0.1461D 00	35.68
v_3	0.1434D 00	0.1914D 00	33.48
v_4	0.1587D 00	0.2167D 00	36.54
t_1	0.3198D-02	0.3417D-02	6.84
t_2	0.5602D-02	0.6141D-02	9.61
t_3	0.7138D-02	0.7883D-02	10.44
t_4	0.7659D-02	0.8496D-02	10.92
θ_1	0.5094D-04	0.1034D-03	102.90
θ_2	0.9327D-04	0.1778D-03	90.58
θ_3	0.1205D-03	0.2155D-03	78.91
θ_4	0.1304D-03	0.2457D-03	88.42

TABLE 13. SQUARE ROOT OF SUM OF SQUARES RESULTS

DISPLACEMENT COORDINATE	TIME HISTORY	ESTIMATE	PERCENT ERROR
r_0	0.1096D-01	0.1277D-01	16.48
v_0	0.1430D-01	0.1277D-01	-10.72
t_0	0.1044D-01	0.1033D-01	-1.03
Ψ_x	0.3547D-04	0.3139D-04	-11.50
Ψ_y	0.2765D-04	0.3139D-04	13.53
r_1	0.4129D-02	0.6305D-02	52.70
r_2	0.8327D-01	0.9610D-01	15.41
r_3	0.1118D 00	0.1272D 00	13.78
r_4	0.1240D 00	0.1405D 00	13.22
v_1	0.5755D-01	0.5187D-01	-9.87
v_2	0.1076D 00	0.9610D-01	-10.72
v_3	0.1434D 00	0.1272D 00	-11.33
v_4	0.1587D 00	0.1405D 00	-11.51
t_1	0.3198D-02	0.3274D-02	2.37
t_2	0.5602D-02	0.5764D-02	2.89
t_3	0.7138D-02	0.7326D-02	2.63
t_4	0.7659D-02	0.7859D-02	2.60
θ_1	0.5094D-04	0.7015D-04	37.69
θ_2	0.9327D-04	0.1281D-03	37.33
θ_3	0.1205D-03	0.1667D-03	38.39
θ_4	0.1304D-03	0.1807D-03	38.57

TABLE 14. DOUBLE SUM RESULTS

DISPLACEMENT COORDINATE	TIME HISTORY	ESTIMATE	PERCENT ERROR
r_0	0.1096D-01	0.1129D-01	2.99
v_0	0.1430D-01	0.1418D-01	-0.79
t_0	0.1044D-01	0.1033D-01	-1.00
Ψ_x	0.3547D-04	0.3490D-04	-1.61
Ψ_y	0.2765D-04	0.2738D-04	-0.97
r_1	0.4129D-02	0.5812D-02	40.76
r_2	0.8327D-01	0.8393D-01	0.79
r_3	0.1118D 00	0.1110D 00	-0.72
r_4	0.1240D 00	0.1225D 00	-1.26
v_1	0.5755D-01	0.5778D-01	0.41
v_2	0.1076D 00	0.1069D 00	-0.67
v_3	0.1434D 00	0.1414D 00	-1.40
v_4	0.1587D 00	0.1562D 00	-1.61
t_1	0.3198D-02	0.3273D-02	2.35
t_2	0.5602D-02	0.5761D-02	2.84
t_3	0.7138D-02	0.7321D-02	2.56
t_4	0.7659D-02	0.7853D-02	2.53
θ_1	0.5094D-04	0.7044D-04	38.26
θ_2	0.9327D-04	0.1283D-03	37.60
θ_3	0.1205D-03	0.1668D-03	38.47
θ_4	0.1304D-03	0.1807D-03	38.61

TABLE 15. CLOSELY SPACED MODES RESULTS

DISPLACEMENT COORDINATE	TIME HISTORY	ESTIMATE	PERCENT ERROR
r_0	0.1096D-01	0.1805D-01	64.68
v_0	0.1430D-01	0.1805D-01	26.23
t_0	0.1044D-01	0.1033D-01	-1.03
Ψ_x	0.3547D-04	0.4438D-04	25.11
Ψ_y	0.2765D-04	0.4438D-04	60.50
r_1	0.4129D-02	0.8916D-02	115.92
r_2	0.8327D-01	0.1359D 00	63.17
r_3	0.1118D 00	0.1798D 00	60.87
r_4	0.1240D 00	0.1986D 00	60.09
v_1	0.5755D-01	0.7333D-01	27.44
v_2	0.1076D 00	0.1359D 00	26.23
v_3	0.1434D 00	0.1798D 00	25.37
v_4	0.1587D 00	0.1986D 00	25.12
t_1	0.3198D-02	0.3274D-02	2.37
t_2	0.5602D-02	0.5764D-02	2.89
t_3	0.7138D-02	0.7326D-02	2.63
t_4	0.7659D-02	0.7859D-02	2.60
θ_1	0.5094D-04	0.7025D-04	37.89
θ_2	0.9327D-04	0.1281D-03	37.38
θ_3	0.1205D-03	0.1667D-03	38.40
θ_4	0.1304D-03	0.1807D-03	38.60

TABLE 16. LIN'S METHOD RESULTS

DISPLACEMENT COORDINATE	TIME HISTORY	ESTIMATE	PERCENT ERROR
r_0	0.1096D-01	0.1791D-01	63.44
v_0	0.1430D-01	0.1791D-01	25.28
t_0	0.1044D-01	0.1033D-01	-1.03
Ψ_x	0.3547D-04	0.4407D-04	24.23
Ψ_y	0.2765D-04	0.4407D-04	59.36
r_1	0.4129D-02	0.8746D-02	111.80
r_2	0.8327D-01	0.1349D 00	62.01
r_3	0.1118D 00	0.1785D 00	59.72
r_4	0.1240D 00	0.1972D 00	58.94
v_1	0.5755D-01	0.7280D-01	26.51
v_2	0.1076D 00	0.1349D 00	25.33
v_3	0.1434D 00	0.1785D 00	24.47
v_4	0.1587D 00	0.1972D 00	24.22
t_1	0.3198D-02	0.3274D-02	2.37
t_2	0.5602D-02	0.5764D-02	2.89
t_3	0.7138D-02	0.7326D-02	2.63
t_4	0.7659D-02	0.7859D-02	2.60
θ_1	0.5094D-04	0.9859D-04	93.53
θ_2	0.9327D-04	0.1801D-03	93.09
θ_3	0.1205D-03	0.2344D-03	94.61
θ_4	0.1304D-03	0.2541D-03	94.86

relatively less significant than lateral motion. These results were to be expected.

Turning to the evaluation of the various response spectrum methods, we find that the results of the absolute sum method, Lin's method, which is similar to the absolute sum method, and the closely spaced modes method, are rather conservative; that is, they overestimate most or all of the maximum displacements. On the other hand, the results of the square root of the sum of the squares method and the double sum method are closer to the time history results but underestimate several displacements. The double sum method, on the whole, gave more accurate results than did the square root of the sum of the squares approach. This is in agreement with the prediction of Rosenblueth and Elorduy, and with the statements by Chu, et al., to the effect that consideration of intermodal coupling leads to an improvement over the square root of the sum of the squares method.

Conclusions

The results of this study are valid for only one particular combination of structural model and excitation. As pointed out by Ts'ao and Werner, the relative merits of the various response spectrum techniques cannot be judged until many more studies of this type are done. If the results of this study were representative of trends supported by many such studies, the following conclusions would be in order:

1. The use of the absolute sum method, Lin's method, or the closely spaced modes method, is highly conservative and leads to costly overdesigning.

2. The use of either the double sum approach or the square root of the sum of the squares approach leads to the underestimation of some maximum displacements and cannot be recommended.
3. To insure that no maximum displacements are underestimated, and to minimize overdesigning, it is recommended that the maximum system displacements be computed by the square root of the sum of the squares method and these results multiplied by 1.2. (This compensates for up to 15% underestimation.)

Despite the superiority of the double sum approach, the square root of the sum of the squares method would be recommended because it is computationally the simpler of the two.

It should be emphasized that the results of this study cannot be generalized. The accuracy of response spectrum techniques cannot help but vary from case to case. Thus, where Lin[2] found his method to be an improvement over the square root of the sum of the squares approach, this study finds the opposite. For this reason, the comments of Lin[11] concerning the sufficiency of conservatism in seismic design, and the argument by Chu, et al., for the adoption of a particular technique for all cases are questionable. Should future studies provide reliable estimates of the upper and lower bounds of the errors in response spectrum techniques, one particular method may indeed emerge as the best. But that situation is not yet upon us.

LIST OF REFERENCES

LIST OF REFERENCES

1. Ts'ao, H. S. and S. D. Werner, Topical Report - Direction of Approach of Seismic Input Motions and Superposition of Modal and Directional Dynamic Responses, TOP-AA105, Agbabian Associates, El Segundo, California, May 1975.

2. Lin, C. W., "On the Simultaneous Application of the Vertical and Horizontal Response Spectra in the Seismic Analysis," Nuclear Engineering and Design, 24, North-Holland Publishing Company, 1973, pp. 232-38.

3. Przemieniecki, J. S., Theory of Matrix Structural Analysis, McGraw-Hill Book Co., New York, 1968.

4. Rubinstein, M. F., Matrix Computer Analysis of Structures, Prentice-Hall, Inc., Englewood Cliffs, New Jersey, 1966.

5. Meirovitch, L., Analytical Methods in Vibrations, The Macmillian Co., New York, 1967.

6. Caughey, T. K., "Classical Normal Modes in Damped Linear Dynamic Systems," Journal of Applied Mechanics, 27, 1960, pp. 269-71.

7. Hurty, W. C. and M. F. Rubinstein, Dynamics of Structures, Prentice-Hall, Inc., Englewood Cliffs, New Jersey, 1964.

8. Chu, S. L., M. Amin, and S. Singh, "Spectral Treatment of Actions of Three Earthquake Components of Structures," Nuclear Engineering and Design, 21, North-Holland Publishing Company, 1972, pp. 126-36.

9. Rosenblueth, E. and J. Elorduy, "Responses of Linear Systems to Certain Transient Disturbances," Paper No. A-1, Proceedings of the Fourth World Conference on Earthquake Engineering, Santiago, Chile, January 1969, pp. 185-96.

10. U.S. Atomic Energy Commission (USAEC), "Combination of Modes and Spatial Components in Seismic Response Analysis," in Regulatory Guide 1.92, Washington, D.C., December 1974.

11. Lin, C. W., "On Spectral Treatment of Actions of Three Earthquake Components on Structures," Nuclear Engineering and Design, 24, North-Holland Publishing Company, 1973, pp. 239-41.

APPENDIX

FØRTRAN LISTING OF MSESM

```
      IMPLICIT REAL*8(A-H,O-Z)
      REAL*4 SNGL
      DIMENSION XDD(3),ETAD(50),ETA(50)
      COMMON/ONE/PHI(50,50),WN(50),GAM(3,50),TIME,STEP,DT,DELT,
     >MODE,NDOF
      COMMON/TWO/ACC(3,2048),ALFA(10),NDIM
      COMMON/TRE/ZETA
      COMMON/FOR/Q(50),QMAX(50)
      DATA ETA,ETAD/100*0.D0/
      PI=3.14159265D0
C
C   READ IN STRUCTURAL DATA AND INTEGRATION PARAMETERS
C
      CALL INPUT
      DO 5 I=1,NDOF
      QMAX(I)=0.D0
    5 CONTINUE
C
C   INPUT GROUND MOTION
C
      CALL XCITE
      IF(NDOF .EQ. 1) GO TO 70
C
C   FOR MULTIPLE DOF SYSTEM,DO TIME HISTORY ANALYSIS FOR
C   SIMULTANEOUS APPLICATION OF ALL COMPONENTS OF GROUND
C   ACCELERATION
C
      QUOT=TIME/DT
      NTIMES=IFIX(SNGL(QUOT))
      DO 50 J=1,NTIMES
C
C   COMPUTE BEGINNING AND ENDING TIMES OF INTERVAL OVER
C   WHICH ALL MODAL EQUATIONS ARE TO BE INTEGRATED BEFORE
C  NEXT CONVERSION TO SYSTEM COORDINATES
C
      TE=DFLOAT(J)*DT
      TB=DFLOAT(J - 1)*DT
      DO 20 I=1,MODE
      T=TB
C
C   COMPUTE INTEGRATION TIME STEP FOR THIS MODAL EQUATION
C
      H=2.D0*PI/WN(I)/STEP
      QUOT=DT/H
      NSTEP=IFIX(SNGL(QUOT))
C
C   COMPUTE GROUND ACCELERATION AT BEGINNING OF INTEGRATION
C   STEP
```

```
      CALL INTRP(T,XDD,DELT)
      DO 10 K=1,NSTEP
      P=0.D0
C
C   COMPUTE MODAL EXCITATION
C
      DO 6 KP=1,3
      P=P - GAM(KP,I)*XDD(KP)
    6 CONTINUE
C
C   INTEGRATE TO NEXT TIME
C
      CALL RK4(H,T,ETA(I),ETAD(I),P,WN(I))
C
C   INCREMENT TIME
C
      T=TB + DFLOAT(K)*H
   10 CONTINUE
C
C   THIS NEXT LITTLE SECTION BRINGS THE INTEGRATION FROM
C   THE END OF THE LAST INTEGRATION STEP FOR THIS MODAL
C   EQUATION TO THE NEXT TIME FOR CONVERSION TO SYSTEM
C   COORDINATES
C
      IF(T .EQ. TE) GO TO 20
      H=TE - T
      CALL INTRP(T,XDD,DELT)
      P=0.D0
      DO 15 KP=1,3
      P=P - GAM(KP,I)*XDD(KP)
   15 CONTINUE
      CALL RK4(H,T,ETA(I),ETAD(I),P,WN(I))
   20 CONTINUE
C
C   CONVERT TO SYSTEM COORDINATES
C
      DO 12 I=1,NDOF
      Q(I)=0.D0
      DO 11 K=1,MODE
      Q(I)=Q(I) + PHI(I,K)*ETA(K)
   11 CONTINUE
   12 CONTINUE
C
C   KEEP TRACK OF MAXIMUM VALUES OF SYSTEM COORDINATES
C
      CALL MAXQ(NDOF)
   50 CONTINUE
C
C   OUTPUT MAX VALUES OF SYSTEM COORDINATES
```

```
      WRITE(6,100)
      DO 60 I=1,NDOF
      WRITE(6,125) QMAX(I)
      WRITE(7,145) QMAX(I),I
   60 CONTINUE
C     STOP
C
      GO TO 999
C
C     FOR A SINGLE DOF SYSTEM, COMPUTE SPECTRAL VALUES FOR
C     NDIM COMPONENTS OF GROUND ACCELERATION
C
C
C     COMPUTE INTEGRATION TIME STEP
C
   70 H=2.D0*PI/WN(1)/STEP
      T=0.D0
      DO 80 I=1,45000
      IF(T .GT. TIME) GO TO 90
C
C     COMPUTE GROUND ACCELERATION
C
      CALL INTRP(T,XDD,DELT)
      DO 75 J=1,NDIM
C
C     COMPUTE MODAL EXCITATION
C
      P=-1.D0*XDD(J)
C
C     INTEGRATE
C
      CALL RK4(H,T,ETA(J),ETAD(J),P,WN(1))
      Q(J)=ETA(J)
   75 CONTINUE
C
C     KEEP TRACK OF MAX VALUES OF MODAL COORDINATES
C
      CALL MAXQ(NDIM)
C
C     INCREMENT TIME
C
      T=DFLOAT(I)*H
   80 CONTINUE
      WRITE(6,110)
      GO TO 999
   90 CONTINUE
```

```
C
C   OUTPUT MAX VALUES OF MODAL COORDINATES
C
      IF(NDIM .EQ. 1) GO TO 95
      WRITE(6,105) (QMAX(I),I=1,3)
      WRITE(7,140) (QMAX(I),I=1,3),MODE
      GO TO 999
   95 WRITE(6,130) QMAX(1)
      WRITE(7,145) QMAX(1),MODE
  100 FORMAT(1H0,'THIS IS IT '/////)
  105 FORMAT(1H0,'MODAL MAXIMA:',T28,D11.4,T58,D11.4,T88,D11.4)
  110 FORMAT(1H0,'NOT YET.')
  120 FORMAT(1H0,D20.10)
  125 FORMAT(1H ,10X,F20.5)
  130 FORMAT(1H0,'MODAL MAXIMUM:',3X,D11.4)
  140 FORMAT(3D20.10,T74,'MM ',I2)
  145 FORMAT(D20.10,T74,'MM ',I2)
  999 STOP
      END
```

```
      SUBROUTINE INPUT
C
C    INPUT STRUCTURAL DATA AND INTEGRATION PARAMETERS
C
      IMPLICIT REAL*8(A-H,O-Z)
      REAL*4 SNGL
      COMMON/ONE/PHI(50,50),WN(50),GAM(3,50),TIME,STEP,DT,DELT,
     >MODE,NDOF
      COMMON/TRE/ZETA
      READ(5,100) TIME,STEP,ZETA,DT,DELT,NDOF,NPC,MODE
      PETA=1.D2*ZETA
      ISTEP=IFIX(SNGL(STEP))
      WRITE(6,105) NDOF,PETA,ISTEP
      IF(NDOF .EQ. 1) GO TO 30
      L=NDOF/NPC
      DO 20 I=1,NDOF
      DO 10 K=1,L
      M=NPC*K
      MN=M - NPC + 1
      READ(5,110) (PHI(J,I),J=MN,M)
   10 CONTINUE
      READ(5,120) WN(I),(GAM(J,I),J=1,3)
      WRITE(6,160) (GAM(J,I),J=1,3)
   20 CONTINUE
      GO TO 99
   30 READ(5,120) WN(1),(GAM(J,1),J=1,3)
      WRITE(6,170) MODE
      WRITE(6,140) WN(1)
      WRITE(6,150)
      WRITE(6,160) (GAM(J,1),J=1,3)
   99 RETURN
      END
```

```
      SUBROUTINE XCITE
C
C    READ IN NDIM COMPONENTS OF DIGITIZED GROUND ACCELERATION
C
      IMPLICIT REAL*8(A-H,O-Z)
      COMMON/TWO/ACC(3,2048),ALFA(10),NDIM
      READ(5,100) NPC,N,NDIM
      IF(NDIM .NE. 1) GO TO 5
      READ(5,125) NAX
      WRITE(6,130) NAX
    5 DO 20 I=1,NDIM
      READ(5,110) (ALFA(J),J=1,10)
      DO 10 K=1,N
      L=K*NPC
      LM=L - NPC + 1
      READ(5,120) (ACC(I,J),J=LM,L)
   10 CONTINUE
   20 CONTINUE
  100 FORMAT(3I5)
  110 FORMAT(10A8)
  120 FORMAT(8F10.0)
  125 FORMAT(A4)
  130 FORMAT(1HO,'GROUND MOTION AXIS:',A4)
      RETURN
      END
      SUBROUTINE INTRP(T,XDD,DELT)
C
C    FIND COMPONENTS OF CURRENT GROUND ACCELERATION BY LINEAR
C    INTERPOLATION
C
      IMPLICIT REAL*8(A-H,O-Z)
      REAL*4 SNGL
      DIMENSION XDD(3)
      COMMON/TWO/ACC(3,2048),ALFA(10),NDIM
      IF(T .NE. 0.DO) GO TO 10
      DO 5 I=1,3
      XDD(I)=0.DO
    5 CONTINUE
      GO TO 99
   10 DO 40 I=1,NDIM
      QUOT=T/DELT
      J=IFIX(SNGL(QUOT))
      IF(J .EQ. 0) GO TO 30
      TX=DFLOAT(J)*DELT
      XDD(I)=ACC(I,J) + (ACC(I,J+1) - ACC(I,J))*(T - TX)/DELT
      XDD(I)=XDD(I)/12.DO
      GO TO 40
   30 XDD(I)=ACC(I,1)*T/DELT
      XDD(I)=XDD(I)/12.DO
   40 CONTINUE
   99 RETURN
      END
```

```
      SUBROUTINE RK4(H,T,X,V,P,WN)
C
C    FOURTH ORDER RUNGE-KUTTA INTEGRATION
C
      IMPLICIT REAL*8(A-H,O-Z)
      COMMON/TRE/ZETA
      FN(X,V)=P - WN**2*X - 2.D0*ZETA*WN*V
      C1=H*FN(X,V)
      T2=T + H/2.D0
      X2=X + H*V/2.D0
      V2=V + C1/2.D0
      C2=H*FN(X2,V2)
      T3=T2
      X3=X2 + H*C1/4.D0
      V3=V + C2/2.D0
      C3=H*FN(X3,V3)
      T4=T + H
      X4=X + H*V + H*C2/2.D0
      V4=V + C3
      C4=H*FN(X4,V4)
      X=X + H*V + H*(C1 + C2 + C3)/6.D0
      V=V + (C1 + 2.D0*C2 + 2.D0*C3 + C4)/6.D0
      RETURN
      END
      SUBROUTINE MAXQ(N)
C
C    KEEP TRACK OF MAX VALUES OF Q
C
      IMPLICIT REAL*8(A-H,O-Z)
      COMMON/FOR/Q(50),QMAX(50)
      DO 10 I=1,N
      A=DABS(Q(I))
      B=DABS(QMAX(I))
      IF(A .GT. B) QMAX(I)=Q(I)
   10 CONTINUE
  999 RETURN
      END
```

VITA

Joseph A. M. Boulet was born in Cass Lake, Minnesota, on July 1, 1948. He graduated from Oak Ridge High School, Oak Ridge, Tennessee, in June 1966, and served with the United States Navy from May 1969 to July 1971.

In June 1975, the author received a Bachelor of Science in Engineering Science degree from the University of Tennessee, Knoxville. That same spring, he was awarded a three year graduate fellowship by the National Science Foundation. He received a Master of Science in Engineering Science from the University of Tennessee, Knoxville, in August 1976.